Theoretical approach on the CLC performance with solid fuels: optimizing the solids inventory

Ana Cuadrat, Alberto Abad[*]*, Pilar Gayán, Luis F. de Diego, Francisco García-Labiano, Juan Adánez*

Instituto de Carboquímica (ICB-CSIC), Dept. of Energy & Environment, Miguel Luesma Castán, 4, Zaragoza, 50018, Spain

[*] Corresponding author: Tel: (+34) 976 733 977. Fax: (+34) 976 733 318. E-mail address: abad@icb.csic.es (A. Abad)

Abstract

Chemical-Looping Combustion (CLC) is a combustion technology with inherent separation of the greenhouse gas CO_2. CLC is considered to be an option with low energy penalty and low cost for CO_2 capture. An option for use CLC with solid fuels is the in-situ Gasification-CLC (iG-CLC), where the solid fuel gasification and the oxidation of gaseous products, i.e. volatile matter and gasification products, simultaneously take place in the fuel reactor of the CLC system.

The objective of this work was to optimize the operating conditions for direct CLC with solid fuels using ilmenite as oxygen carrier. A simplified model for the fuel reactor has been developed, which describes the complex processes happening in the fuel reactor. Thus, the effect of the main operating variables in the iG-CLC process can be analyzed in a simpler way than using a detailed model. The model includes the possibility of using a carbon separation system to recirculate unreacted char particles exiting from the fuel reactor, reducing the by-pass of carbon to the air reactor. Also, the gasification kinetics of a bituminous coal for both H_2O and CO_2 as gasification agents and the kinetics of the reduction reaction of ilmenite with H_2, CO and CH_4 are incorporated to the model. First, the simulated results have been compared to experimental results from tests performed in a continuous 500W_{th} CLC plant. Later, model simulations were performed to evaluate the effect of the main operating variables of the fuel reactor (e.g. temperature, solids inventory, efficiency of the carbon separation system, oxygen carrier to fuel ratio, or flow and type of gasification agent) on the combustion and carbon

capture efficiencies. The carbon capture was directly related to the extent of gasification, which is promoted by increasing the temperature or the residence time of char particles in the fuel reactor. It is highly beneficial to increase the solids inventory up to 1000 kg/MW_{th}, but further increase does not give a relevant improvement in the carbon capture and it is better to increase the carbon separation efficiency than the solids inventory. With an inventory of 1000 kg/MW_{th}, at 1000ºC and a carbon separation efficiency of 90% the carbon capture predicted was 86.0%.

1. Introduction

Chemical-Looping Combustion (CLC) is a novel combustion technology with inherent separation of the greenhouse gas CO_2 that involves the use of an oxygen carrier, that transfers oxygen from air to the fuel avoiding the direct contact between them. Commonly, the CLC system is made of two interconnected reactors, designated as air and fuel reactors. In the fuel reactor, the fuel is oxidized to CO_2 and H_2O by an oxygen carrier that is reduced. The reduced oxygen carrier is further transferred into the air reactor where it is oxidized with air, and the material regenerated is ready to start a new cycle. The flue gas leaving the air reactor contains N_2 and unreacted O_2. The exit gas from the fuel reactor contains only CO_2 and H_2O. After water condensation, almost pure CO_2 can be obtained with little energy lost and low cost [1,2].

The CLC process has been widely developed for gaseous fuels [3]. However, it could be advantageous if the CLC process could be adapted to the use of solid fuels. One of the options to use the CLC technology with solid fuels is the so-called in-situ gasification Chemical-Looping Combustion (iG-CLC) [3]. In this technology the solid fuel is introduced directly in the CLC system and thereby coal gasification and reaction of the released volatile matter and gasification products with the oxygen carrier take place simultaneously in the fuel reactor. In the iG-CLC process the fuel reactor is fluidized by a gasifying agent, e.g., H_2O or CO_2, as proposed by Cao et al. [4]. Thereby, the solid fuel devolatilization and gasification takes place in the fuel reactor first and the resulting gases and volatiles are oxidized through reduction of the oxidized oxygen carrier, Me_xO_y. The oxygen carrier reduced in the fuel reactor, Me_xO_{y-1}, is subsequently led to the air reactor where it is re-oxidized with air. The net chemical reaction as well as the heat involved in the global process is the same as for usual combustion.

Fig. 1 shows the simplified reactor scheme of the CLC process with direct introduction of solid fuels, which is composed by an air and a fuel reactor and the oxygen carrier that circulates between them. Experimentally it was found that working at high temperatures is required to reach high gasification rates [5]. The gasification process was found to be the most relevant step to achieve high carbon capture as the solids stream going out from the fuel reactor can contain certain fraction of unconverted char [6]. Thus, the implementation of a carbon separation system is fundamental to ensure high gasification extent and thus high carbon capture. Simple calculations done in a previous work have shown that a carbon separation system is a critical component in order to have high carbon capture efficiency [7]. A carbon stripper has been proposed in the literature as the carbon separation system [4]. The carbon stripper increases the residence time of char in the fuel reactor by separating and reintroducing ungasified char particles exiting the fuel reactor [4,6].

To use an oxygen carrier with adequate behavior and properties is fundamental to reach high performance in the CLC process. As for this option of CLC with solid fuels, the fuel is physically mixed with the oxygen carrier, being predictable a partial loss of oxygen carrier particles together with the draining stream of coal ashes to avoid their accumulation in the system. In this context, the use of low cost materials such as natural minerals or industrial waste products as oxygen carriers turns out to be very interesting [6-12]. Among them, ilmenite is a low cost natural mineral which is promising for its large scale industrial use as oxygen carrier with solid fuels. Performance of ilmenite has been proven to be acceptable as oxygen carrier for CLC in recent studies made at different scales [13,14]. Comparing the performance of several natural iron ores and industrial products, Norwegian ilmenite was ranked among the materials which showed higher reactivity for both gaseous and solid fuels [9,10]. Although ilmenite particles initially have a rather low reactivity, it undergoes an activation process after several redox cycles, where its reactivity remarkably increases for H_2, CO and CH_4 as reacting gases [14]. The gas conversion showed by activated ilmenite was even similar to one synthetic $Fe_2O_3/MgAl_2O_4$ material selected from previous works [15]. Ilmenite has high conversion of CO and H_2 for syngas applications, but moderate conversion of CH_4 for the use of natural gas as fuel [14]. On the whole, ilmenite has adequate values of reactivity and oxygen transport capacity for its use in the CLC technology with solid fuels, which is confirmed by the results from the continuous CLC experiments done to

date. Additionally, ilmenite showed good mechanical stability and good fluidizing properties [16].

In order to optimize the iG-CLC system the modeling of the process is needed. A summary of the mechanisms to date used for the modeling of CLC with solid fuels can be found in Adánez et al. [3]. There is little modeling work done in CLC with solid fuels. Mahalatkar et al. [17] simulated the behavior of a small batch fluidized bed for coal conversion using a Fe-based oxygen carrier. They used the gasification kinetics and the reduction kinetics of the oxygen carrier with pyrolysis and gasification products. The theoretical results agreed to the experimental results. The combustion efficiency depends on the char conversion in the fuel reactor and on the reactivity of the oxygen carrier with the volatiles and gasification gases [5]. In addition, Ströhle et al. [18] presented a simulation of 1 MW_{th} iG-CLC unit. They showed the need of a carbon separation system in order to reach high values of char conversion in the fuel reactor because of the slow gasification reaction.

The objective of this work was to determine the operating conditions that optimize the carbon capture and combustion efficiencies in a CLC system fuelled with coal. For that, a simplified model based on mass balances of a CLC system, including chemical reactions and flow patterns, has been developed. Ilmenite was selected as oxygen carrier and a bituminous Colombian coal "El Cerrejón" as solid fuel. In order to prove the validity of the model, the results predicted with this model were compared to experimental tests done in a 500 W_{th} unit with this type of fuel and this oxygen carrier. Later, the effect of the main operating parameters on the combustion and carbon capture efficiency of the CLC system was analyzed. The parameters considered were the solids inventory, the fuel reactor temperature, the efficiency of the carbon separation system, the oxygen carrier to fuel ratio, the reduction degree of the oxygen carrier, the type and flow of gasification agent, the fraction of oxygen carrier in contact with the volatile matter, and the oxygen carrier reaction rate.

2. Reacting scheme in the fuel reactor

A theoretical model is a very useful tool to understand the operation of the system in a general way, as well as to predict the influence of the different variables and optimize their values. In this section a theoretical model for the fuel reactor has been developed based on a simple reacting scheme. The model was as simple as possible, but describing

with accuracy the complex chemical processes happening in the fuel reactor. Thus, the effect of the main operating variables in the iG-CLC process can be analyzed in a simpler way than using a more complete description of the gas and solids flow pattern in the reactor.

The flow patterns of gas and solids here assumed were based on results obtained in a continuously operated CLC unit [5,12]. In these experimental works, it was found that the unconverted CH_4, CO and H_2 from the fuel reactor were mainly coming from unconverted volatile matter. However, neither tars nor other hydrocarbons than CH_4 were found. Also, gasification products were highly converted to CO_2 and H_2O. A bad contact between volatile matter and oxygen carrier particles was proposed as the main reason for incomplete combustion.

Based on these results, a model of the system was developed to predict and optimize the combustion and carbon capture efficiencies of the CLC process as a function of various operational parameters. Thus, two different gaseous flows in the reactor are considered independently and in plug flow: one for the gasification products in the dense phase and another for the volatile matter released in plume. Fig. 2 shows a scheme of this flow pattern. To simulate the different contact between the released gaseous fuels, the oxygen carrier bed in the fuel reactor was considered to be divided into two separated zones: one zone is in contact with the volatiles and the other zone reacts with the generated gasification products. It is considered that there is perfect mixing of the solids and no constrictions for the gas-solid reactions. Thus, this model assumes that there is no gas exchange between the generated flow of gasification products in the dense bed and volatile plume. Also, the model assumes that the only reducing species in the dense bed are H_2 and CO, whereas CH_4 also appears in the flow coming from the volatile plume.

The model was developed and applied to ilmenite as oxygen carrier and El Cerrejón coal as fuel. Calculations were made on the basis of 1 MW_{th} of corresponding fuel power. The ultimate and proximate analyses and the heating value of the fuel are gathered in Table 1. The simulations with variation of different parameters were done using the properties of the fresh coal. However, the first simulations were done using the pre-treated coal as fuel, since their results were used to compare and validate the model with experimental results which were done with coal that was pre-treated to eliminate some agglomeration problems that were observed in this coal [5]. Neither sulfur nor nitrogen present in the fuel were considered in this model.

For the development of the model, it is necessary to know (1) the reaction scheme to be considered in the mass balance; (2) the content and composition of the volatile matter in coal, (3) the kinetics of char gasification with the gasification agent used; and (4) the kinetics of the subsequent reaction of the gasification products with the oxygen carrier together with the kinetics of the later reaction of the volatile matter with the oxygen carrier are also required.

2.1. Differential mass balances in the fuel reactor

The mass flow changes in a differential mass of the reactor have been considered in the model. To carry out differential mass balances of reactants and products during reaction, the bed is divided into differential elements, both for (1) the gas flow in the dense phase, where gasification takes place, and (2) the flow of volatile matter. Both flows go in parallel and it was assumed that there is no exchange of gases among them. $F_{i,g,1}$ and $F_{i,g,2}$ are the gas flows of the gasification product i at the inlet and outlet of the compartment in the dense phase, respectively; and $F_{i,v,1}$ and $F_{i,v,2}$ are the gas flows of the released gas i in the volatiles at the inlet and outlet of the inventory differential mass, respectively.

The mass balance in a differential mass is defined according to the following scheme of reactions happening simultaneously in the fuel reactor:

$$\text{Coal} \rightarrow \text{a CO} + \text{b } H_2 + \text{c } CH_4 + \text{d } H_2O + \text{e } CO_2 + \text{f C (Char)} \quad (1)$$

$$\text{C (Char)} + H_2O \rightarrow CO + H_2 \quad (2)$$

$$\text{C (Char)} + CO_2 \rightarrow 2\ CO \quad (3)$$

$$Me_xO_y + CH_4 \rightarrow Me_xO_{y-1} + CO + 2\ H_2 \quad (4)$$

$$Me_xO_y + H_2 \rightarrow Me_xO_{y-1} + H_2O \quad (5)$$

$$Me_xO_y + CO \rightarrow Me_xO_{y-1} + CO_2 \quad (6)$$

$$2\ Me_xO_y + \text{C (Char)} \rightarrow 2\ Me_xO_{y-1} + CO_2 \quad (7)$$

$$CO + H_2O \leftrightarrow CO_2 + H_2 \quad (8)$$

Eq. (1) represents the coal devolatilization. Coefficients *a* to *e* depend on the distribution of gases generated during the devolatilization in steam-CO_2 mixtures, whose correlation used in this model will be described in section 2.2. Eqs. (2) and (3) show the char gasification with steam and CO_2, and Eqs. (4) to (6) represent the

oxidation of the products of coal devolatilization and gasification by the oxygen carrier, i.e. only H_2, CO and CH_4 are considered as reducing species. The reduction of ilmenite with solid carbon through a true solid-solid reaction is represented in Eq. (7). However, results obtained in fluidized-bed reactors showed that the reduction by gasification products, i.e. H_2 and CO, had a higher relevance than the direct solid-solid reaction [7,20,21]. Therefore, the solid-solid reaction was not included in the model.

Eq. (7) corresponds to the Water-Gas Shift reaction. The fulfillment of it could modify the CO, H_2, H_2O and CO_2 final concentrations. However, previous CLC experiments performed with solid fuels show that the outlet concentrations are not in equilibrium and that the Water-Gas Shift has no important influence on the gas product composition [16].

Because of the different contact with the oxygen carrier and location of generation, the reaction of the volatile matter species and char gasification products are considered separately in this simplified model. Therefore, the mass balances for the H_2 and CO generated in the dense bed from char gasification are expressed by Eq. (9) and (10), respectively. For the volatile matter released reducing species, i.e., CH_4, H_2 and CO, the mass balances are Eqs. (13), (14) and (15). These equations show the variation of the molar flows of H_2, CO and CH_4 - F_{H_2}, F_{CO} and F_{CH_4}, respectively-, for the gasification and devolatilization products in a bed differential mass inventory dm_{OC}.

Mass balances in dense bed:

$$\frac{\partial F_{H_2}}{\partial m_{OC}} + \left[\frac{1}{2d \cdot M_O} (-r_{ilm,H_2})(1-\chi_{OC,v}) - \frac{f_C}{1-f_C} (r_{gasif})_{H_2O} \frac{1}{M_C} \right] = 0 \quad (9)$$

$$\frac{\partial F_{CO}}{\partial m_{OC}} + \left[\frac{1}{2d \cdot M_O} (-r_{ilm,CO})(1-\chi_{OC,v}) - \frac{f_C}{1-f_C} (r_{gasif})_{H_2O} \frac{1}{M_C} - 2\frac{f_C}{1-f_C} (r_{gasif})_{CO_2} \frac{1}{M_C} \right] = 0 \quad (10)$$

$$\frac{\partial F_{H_2O}}{\partial m_{OC}} + \left[-\frac{1}{2d \cdot M_O} (-r_{ilm,H_2})(1-\chi_{OC,v}) + \frac{f_C}{1-f_C} (r_{gasif})_{H_2O} \frac{1}{M_C} \right] = 0 \quad (11)$$

$$\frac{\partial F_{CO_2}}{\partial m_{OC}} + \left[-\frac{1}{2d \cdot M_O} (-r_{ilm,CO})(1-\chi_{OC,v}) + \frac{f_C}{1-f_C} (r_{gasif})_{CO_2} \frac{1}{M_C} \right] = 0 \quad (12)$$

Mass balances in volatile plume:

$$\frac{\partial F_{CH_4}}{\partial m_{OC}} + \frac{1}{2d \cdot M_O} (-r_{ilm,CH_4}) \cdot \chi_{OC,v} = 0 \quad (13)$$

$$\frac{\partial F_{H_2}}{\partial m_{OC}} + \frac{1}{2d \cdot M_O}(-r_{ilm,H_2}) \cdot \chi_{OC,v} + 2\frac{\partial F_{CH_4}}{\partial m_{OC}} = 0 \quad (14)$$

$$\frac{\partial F_{CO}}{\partial m_{OC}} + \frac{1}{2d \cdot M_O}(-r_{ilm,CO}) \cdot \chi_{OC,v} + \frac{\partial F_{CH_4}}{\partial m_{OC}} = 0 \quad (15)$$

$$\frac{\partial F_{H_2O}}{\partial m_{OC}} - \frac{1}{2d \cdot M_O}(-r_{ilm,H_2}) \cdot \chi_{OC,v} = 0 \quad (16)$$

$$\frac{\partial F_{CO_2}}{\partial m_{OC}} - \frac{1}{2d \cdot M_O}(-r_{ilm,CO}) \cdot \chi_{OC,v} = 0 \quad (17)$$

It was assumed that the coal devolatilization takes place instantaneously at the coal feeding level. The contour conditions for the dense bed and plume phase are described by Eqs. (18) and (19), respectively, which are defined at $m_{OC} = 0$, that is, at the bottom of the fuel reactor:

$$F_j = F_{j,gas}^0 \quad (18)$$

$$F_k = F_{k,vol}^0 \quad (19)$$

where F_j is the flow of the gas component j in the dense bed and $F_{j,gas}^0$ is the flow of the gas j introduced as gasification agent -usually H_2O or CO_2. F_k is the flow of the gas component k in the plume, i.e., CH_4, H_2, CO, H_2O and CO_2, and $F_{k,vol}^0$ is the flow of the gas component k that is released when coal is devolatilized at the bottom of the fuel reactor.

Char is assumed to be uniformly distributed throughout the bed in perfect mixing. Thus, the carbon concentration in the bed, f_C, has a constant value throughout the reactor. The gasification rate, r_{gas}, is based per mass of carbon in char. But the mass balances in the dense bed are formulated per mass of oxygen carrier; see Eqs (9-12). Thus, the term $f_C/(1-f_C)$ in these equations is necessary to express the gasification rate per mass of oxygen carrier in a differential element, being congruent with the formulation of the equations. The gasification takes place simultaneously with the reaction of the released volatile matter and gasification products with ilmenite. $(-r_{ilm,H_2})$, $(-r_{ilm,CO})$ and $(-r_{ilm,CH_4})$ are the reaction rates of ilmenite with H_2, CO and CH_4, respectively. The gasification products are generated in the dense bed and they have good contact with the

oxygen carrier particles and are considered to react separately from the volatiles. The volatiles are released in a plume and they get in poorer contact with the oxygen carrier. To take this into account, the oxygen carrier bed is considered to be separated in two zones and the parameter $\chi_{OC,v}$ is introduced as the fraction of the oxygen carrier bed that is in contact with the volatile matter.

The global balance to the whole reactor is done by integrating the differential equations over the total bed mass inventory. To solve the system of simultaneous differential equations, the Runge–Kutta–Merson method was used. Initially, a value of ΔX_s and f_C is assumed. Thus, the values of the flows of H_2, CO, CH_4, CO_2 and H_2O outgoing the reactor are obtained. From these values new values of ΔX_s and f_C are obtained. An iterative method is used until both parameters converged to obtain the solution to the mathematical model.

From experimental results obtained in continuously operated units [5,12] it was concluded that the implementation of a carbon separation system seemed to be essential to obtain high carbon capture in an iG-CLC process. The carbon separation system separates un-gasified char from oxygen carrier particles exiting from the fuel reactor, to be later reintroduced to the fuel reactor. Thereby the fraction of carbon by-passed to the air reactor, which will be burnt and not captured, is reduced. The use of a highly efficient carbon separation system ensures high extent of gasification, and thereby high carbon capture, by increasing char residence time in the fuel reactor. In Fig. 3 a scheme of carbon flows involved in the fuel reactor and carbon separation system is represented. The efficiency of the carbon separation system, η_{CS}, on the carbon capture efficiency has been evaluated in this work. η_{CS} is defined as the fraction of carbon in char that is separated and recirculated back to the fuel reactor with respect to the carbon in the char that exits the fuel reactor together with the flow of oxygen carrier particles.

$$\eta_{CS} = 1 - \frac{F_{CO_2,AR}}{\left(F_{C,char}\right)_{out}} \tag{20}$$

$\left(F_{C,char}\right)_{out}$ is the molar flow of carbon in char exiting the fuel reactor:

$$\left(F_{C,char}\right)_{out} = \frac{\dot{m}_{OC} \cdot f_C / M_C}{(1 - f_C)} \tag{21}$$

$\dot{m}_{OC}$ is the solids recirculation rate, which is the oxygen carrier flow in the fuel reactor. Thus, the calculated carbon capture efficiency will depend on the solids circulation rate. In addition, the carbon not separated by the carbon separation system enters in the air reactor where it gets oxidized to CO_2. This carbon flow, $F_{CO_2,AR}$, is calculated from the mass balance expressed by Eq (22).

$$F_{CO_2,AR} = [C]_{fuel} \cdot \dot{m}_{fuel,in} / M_C - \left[\left(F_{CO_2} + F_{CO} + F_{CH_4} \right)_{out} - \left(F_{CO_2} \right)_{in} \right] \quad (22)$$

The simulation results are obtained after adjusting the carbon fraction in the fuel reactor bed so that the flow of gasification products accomplishes the following mass balances:

$$\left(F_{C,char} \right)_{in} = \left(F_{C,char} \right)_{out} + \left(F_C \right)_{gp} \quad (23)$$

$$\left(F_C \right)_{gp} + \left(F_C \right)_{vol} = \left(F_{CO_2} + F_{CO} + F_{CH_4} \right)_{out} - \left(F_{CO_2} \right)_{in} \quad (24)$$

$\left(F_{C,char} \right)_{in}$ is the carbon flow in char entering the fuel reactor, which is sum of the char in the coal feed and the char recirculated by the carbon separation system; $\left(F_{C,char} \right)_{out}$ is the carbon flow of ungasified char that exits the fuel reactor; $\left(F_C \right)_{gp}$ is the flow of carbon contained in the products of char gasification; and $\left(F_C \right)_{vol}$ is the flow of carbon in volatiles.

Taking into account for the calculation of the carbon flow exiting the fuel reactor, see Eq (21), if the solids circulation rate is increased, the fraction of carbon from char in the fuel reactor, f_C, must decrease to fulfill the carbon balance expressed in Eq. (23). This fact is also considered in the carbon balance in the fuel reactor, expressed in Eqs. (9-12), affecting to the carbon being gasified.

2.2. Solid fuel devolatilization

In this simplified model it was assumed that the devolatilization was instantaneous for the range of coal particle size used and it took place in the bottom part of the bed, since models predict devolatilization times in the order of less than one second under these conditions [22]. All volatile matter was considered to be converted into gaseous species. The composition of volatiles was experimentally obtained from devolatilization of El

Cerrejón coal in a fluidized bed using silica sand as bed material and H_2O or CO_2 as fluidizing gas [5]. In all cases the volatile matter was released in form of H_2, CO, CH_4, H_2O and CO_2 as gaseous species. Also small amounts of light hydrocarbons and tars were found. Table 2 gathers the mass of the main gaseous species found in volatile matter generated from 100 g of El Cerrejón coal for the three different H_2O-CO_2 mixtures. The difference between the released devolatilized species for different fluidizing gas composition is because there is some CH_4 reforming taking place with H_2O and CO_2. Note also that, in some cases of the compositions given the values of H_2O or CO_2 have negative values, because some H_2O and CO_2 was taken from the gasification agent flow for the partial CH_4 reforming.

2.3. Char gasification

In char gasification, whose main component is carbon, the most common gasification agents are steam and CO_2, through which H_2 and CO are generated as for the following reactions (2) and (3).

Kinetics of the gasification reactions for the El Cerrejón coal were obtained by TGA analysis. For kinetics determination, conversion vs. time curves at different temperatures (900-1050ºC), gasification agent concentrations (i.e. 20-80 vol.% H_2O or CO_2) and gas product concentrations (i.e. 0-40 vol.% H_2 or CO) were obtained. A similar procedure was used to those found in [23]. As an example, Fig. 4 shows the char conversion versus time curves for the gasification reactions with H_2O of El Cerrejón coal at different temperatures and different H_2 fractions as inhibitory agent obtained by TGA.

It was assumed that char gasifies according to the homogeneous reaction model with control by chemical reaction. The surface reaction follows a Langmuir-Hinshelwood reaction model [23] and the reaction rate is constant with the char conversion. The gasification rate r_{gasif} is defined by Eq. 32.

$$r_{gasif} = \frac{1}{(1 - X_{char})} \frac{dX_{char}}{dt} = \frac{k_1 p_{react}}{1 + k_2 p_{react} + k_3 p_{prod}} \tag{25}$$

where X_{char} is the char conversion, p_{react} is the partial pressure of the gaseous reactants, i.e. H_2O or CO_2, p_{prod} is the partial pressure of the gasification products, i.e. H_2 or CO, and k_1, k_2 and k_3 are the kinetic constants.

Thus, the gasification kinetic parameters were obtained when using H_2O and CO_2 as gasification agents and taking into account the inhibitory effect of H_2 and CO. The gasification kinetic constants obtained are gathered in Table 3 in case of using H_2O or CO_2 as gasification agent.

2.4. Reaction of ilmenite with devolatilization and gasification products

The oxygen carrier considered in this work is ilmenite. Physical and chemical properties of this material can be found elsewhere [14]. The oxidized ilmenite is a mixture of Fe_2TiO_5 and Fe_2O_3 as the main reacting compounds. The reduced compounds were considered to be $FeTiO_3$ and Fe_3O_4, respectively. The corresponding oxygen transport capacity of ilmenite, $R_{O,ilm}$, was 4 wt.%, which was stated to be invariant in tests in a 500 W_{th} facility [5].

Ilmenite undergoes an activation process and reaches a maximum and stable reaction rate. This activation was seen to occur fast in continuous operation with coal as fuel [5]. Thus, the kinetics for activated ilmenite with H_2, CO and CH_4 has been used for modeling purposes in this work, which were obtained in a previous work by Abad et al. [13].

A changing grain size model, with uniform reaction in the particle and chemical reaction control was assumed. The main equations that describe this model are the following:

$$t/\tau_i = 1-\left(1-X_{s,i}\right)^{1/3} \tag{26}$$

$$\tau_i = \frac{\rho_m r_{grain}}{\overline{b}\cdot k_{s0}\cdot e^{(-E_a/RT)}\cdot C_{g,i}^{n}} \tag{27}$$

τ_i being the time for complete solid conversion of the oxygen carrier for the reduction reaction considered. Table 4 summarizes the kinetic parameters used for the calculation of the reaction of ilmenite with H_2, CO and CH_4, coming from the devolatilization and char gasification. In this case, the reaction of CH_4 with the oxygen carrier is considered to take place by means of a partial oxidation with CO and H_2 as intermediate products,

see Eq. (11), as it has been observed in other studies [24-26]. Thus, the stoichiometric parameter $\bar{b}$ takes the correspondent value for the stoichiometry of reaction (4) with ilmenite, where Fe_2TiO_5 and Fe_2O_3 are reduced to $FeTiO_3$ and Fe_3O_4, respectively.

The reaction rate of ilmenite for a given reaction *i*, $(-r_{ilm,i})$, is calculated as:

$$(-r_{ilm,i}) = \frac{\Phi}{3} R_{O,ilm} \frac{dX_{s,i}}{dt} \tag{28}$$

$X_{s,i}$ being the conversion of ilmenite by the reaction *i* and Φ the characteristic reactivity in the reactor. The parameter Φ takes into account the residence time distribution of particles in the reactor and the reacting time until complete conversion of particles. Assuming perfect mixing of solids in the reactor and reaction of particles following a shrinking core model with spherical geometry, the characteristic reactivity can be calculated as [27]:

$$\Phi = 3\left[1 - \bar{X}_{s,in}^{2/3} \exp\left(-\frac{\left(1-\bar{X}_{s,in}^{1/3}\right)}{\Delta X_s}\Phi_j\right)\right] - \frac{6\Delta X_s}{\Phi}\left[1 - \bar{X}_{s,in}^{1/3} \exp\left(-\frac{\left(1-\bar{X}_{s,in}^{1/3}\right)}{\Delta X_s}\Phi\right)\right] + \frac{6\Delta X_s^2}{\Phi^2}\left[1 - \exp\left(-\frac{\left(1-\bar{X}_{s,in}^{1/3}\right)}{\Delta X_s}\Phi\right)\right] \tag{29}$$

ΔX_s being the variation of solids conversion in the reactor and $X_{s,in}$ the conversion of solids at the reactor inlet. As starting point, the calculations for the model consider that ilmenite is fully oxidized in the air reactor, i.e. the conversion for the reduction reaction is 0.

The variation of the solids conversion in the reactor, ΔX_s, is the oxygen transferred by the oxygen carrier in the fuel reactor to oxidize the fuel divided by the oxygen that can be supplied by the circulating oxygen carrier. So ΔX_s, is calculated as:

$$\Delta X_s = M_O \frac{\left[2F_{CO_2} + F_{CO} + F_{H_2O}\right]_{out} - \left[2F_{CO_2} + F_{H_2O}\right]_{in}}{R_{O,ilm} G_s} \tag{30}$$

G_s being the solids circulation flow rate.

3. Performance evaluation

One of the main parameters to evaluate the performance of a CLC system is the carbon capture efficiency, η_{CC}. This efficiency takes into consideration the physical removal of carbon dioxide that would otherwise be emitted into the atmosphere and it is defined as the fraction of the carbon introduced that is converted to gas in the fuel reactor.

$$\eta_{CC} = M_C \frac{\left(F_{CO_2} + F_{CO} + F_{CH_4}\right)_{out} - \left(F_{CO_2}\right)_{in}}{[C]_{fuel} \cdot \dot{m}_{fuel,in}} \tag{31}$$

$\dot{m}_{fuel,in}$ being the coal feeding flow and $[C]_{fuel}$ the carbon fraction in the fuel. Note that in this technology the char that has not been gasified is by-passed to the air reactor, where is burnt to CO_2 which is not captured.

All the volatiles get out through the fuel reactor, so η_{CC} depends on the gasification efficiency or char conversion, X_{char}, which is the fraction of the carbon in char introduced the fuel reactor, $(F_{C,char})_{in}$, that has been gasified. It is calculated as:

$$X_{char} = \frac{(F_{C,char})_{in} - F_{CO_2,AR}}{(F_{C,char})_{in}} \tag{32}$$

As CLC is a combustion technology, it is fundamental to get high combustion efficiency in the fuel reactor, $\eta_{comb\ FR}$. The combustion efficiency in the fuel reactor is defined as the fraction of the oxygen demanded by the volatile matter and gasification products that is supplied by the oxygen carrier in the fuel-reactor.

$$\eta_{comb\,FR} = \frac{(F_{H_2O} + 2F_{CO_2} + F_{CO})_{out} - (F_{H_2O} + 2F_{CO_2} + F_{CO})_{in}}{\Omega_{coal} - 2F_{CO_2,AR}} \tag{33}$$

Thus, the combustion efficiency in the fuel reactor only considers the combustion of compounds that can be oxidized in the reactor, i.e. gases from volatiles or char gasification. The oxygen supplied by the oxygen carrier, numerator in Eq. (33), is calculated from an oxygen balance to gaseous compounds entering to and exiting from the reactor. The oxygen demanded by gaseous compounds evolved in the fuel reactor, denominator in Eq. (33), is calculated as the oxygen demanded by coal to be fully

oxidized, Ω_{coal}, minus the oxygen demanded by carbon not emitted in the fuel reactor, i.e. $F_{CO_2,AR}$. The oxygen demanded by coal is defined as:

$$\Omega_{coal} = M_O(2[C]_{fuel}/M_C + 0.5[H]_{fuel}/M_H - [O]_{fuel}/M_O)\cdot\dot{m}_{fuel,in} \quad (34)$$

$[C]_{fuel}$, $[H]_{fuel}$ and $[O]_{fuel}$ being the carbon, hydrogen and oxygen fractions in the fuel, whose values are obtained from the proximate analysis.

To evaluate the extent that coal is burned to CO_2 and H_2O in the CLC system, not only in the fuel reactor but also in the air reactor, the oxygen demand is defined. In this case, the oxygen demand is referred here as the oxygen required to fully oxidize the unconverted gases exiting the fuel reactor to CO_2 and H_2O with respect the total oxygen demand of the fuel.

$$\Omega_T = \frac{(F_{H_2} + F_{CO} + 4F_{CH_4})_{out}}{\Omega_{coal}} \quad (35)$$

The performance of the iG-CLC process was evaluated by analyzing these parameters as a function of the residence time of particles in the fuel reactor, which depends on the solids inventory and the solids circulation flow rate. Evaluation of the solids circulation flow rate was done by the use of the oxygen carrier to fuel ratio, ϕ, defined as the availability of oxygen in the flow of oxygen carrier divided by the oxygen required to fully convert the fuel to CO_2 and H_2O:

$$\phi = \frac{R_{O,ilm}\dot{m}_{OC}}{\Omega_{coal}} \quad (36)$$

So, $\phi = 1$ corresponds to the stoichiometric flow of oxygen carrier needed for a full conversion of the fuel to CO_2 and H_2O.

4. Results and discussion

A model has been developed to predict both the carbon capture and combustion efficiencies of the iG-CLC process as a function of various operational parameters with ilmenite as oxygen carrier and a bituminous coal “El Cerrejón” as fuel. The gasification

kinetics of this type of coal including the inhibitory effect of the gasification products, and the reaction kinetics of ilmenite obtained by Abad et al. [13] were included in the model. In addition, the effect of the presence of a carbon separation system is analyzed. The model calculates the gas flow for CO_2, CO, H_2, H_2O and CH_4 exiting from the fuel reactor, as well as the fraction of unconverted char passing to the air reactor. Thus, the carbon capture and combustion efficiency can be evaluated. Firstly, the predictions of the model were checked with experimental results in a 500 W_{th} CLC plant. After that, simulations were performed using the model in order to evaluate the effect of operational parameters on the performance of iG-CLC systems. The operational parameters analyzed were the fuel reactor temperature, the solids inventory, the efficiency of the carbon separation system, the type and flow of gasification agent, the oxygen carrier to fuel ratio, the reduction degree of the oxygen carrier at the inlet of the fuel reactor, the oxygen carrier reaction rate and the fraction of oxygen carrier bed that is in contact with the volatile matter. All simulations performed were made for a corresponding thermal power of 1 MW_{th}, which is a feeding rate of El Cerrejón fresh coal of 0.0386 kg/s.

4.1. Comparison with experimental results

The model results simulated were compared to the experimental results obtained in continuous operation in the 500W_{th} CLC unit placed at the Instituto de Carboquímica operated with pre-treated El Cerrejón bituminous coal and using ilmenite as oxygen carrier. The facility has no carbon separation system. Thus, calculations were done by setting the parameter η_{CS} = 0. The experiments were done at T_{FR} of 900ºC, the corresponding oxygen carrier to fuel ratio ϕ was around 2, steam was used as gasification agent with steam to fixed carbon ratio H_2O/C = 0.7 and the inventory was 3100 kg/MW_{th}. In addition, ilmenite enters in the fuel reactor fully oxidized, i.e. $X_{s,i}$ = 0 [5].

Preliminary results were obtained considering that the whole oxygen carrier bed got in contact with the volatile matter and the gasification products in the dense bed. The first simulations predicted full combustion of the products of devolatilization and gasification. However, the experimental results showed some incomplete combustion, which was found to be due to H_2, CO and CH_4 coming from the volatile matter. As mentioned, the volatile matter was not fully burnt due to poor contact with the oxygen

carrier particles, whereas char gasification products were found to be fully burnt at temperatures above 890ºC, as for the results obtained from experiments fuelled with char from the same coal [5]. Therefore, it was considered that only part of the oxygen carrier bed was in contact with the volatile matter. Thus, a fraction of oxygen carrier in the fuel reactor that is in contact with the volatile matter, $\chi_{OC,v}$, was introduced to predict the experimental fuel reactor combustion efficiencies obtained. Simulations varying $\chi_{OC,v}$ were performed. It was obtained that the $\chi_{OC,v}$ that predicts the combustion efficiencies obtained experimentally at different temperatures is 0.53%. $\chi_{OC,v}$ = 0.53% is a rather low value, that is, the volatile matter released in the plume in the experimental facility had indeed bad contact with the oxygen carrier. Fig. 5 shows a comparison between predicted and experimental fuel reactor combustion efficiencies, considering $\chi_{OC,v}$ = 0.53%. It can be seen that there is a good agreement between the predicted and measured values.

As an example, experimentally at 900ºC the following efficiencies were obtained: η_{CC} = 51.0%, X_{char} = 32.0% and $\eta_{comb\ FR}$ = 90.0% in the 500W_{th} plant. Two simulations with the same operating conditions were done to compare with experimental results. The first one considered that the whole oxygen carrier bed is in contact with both volatile matter and gasification products. With this simulation a combustion efficiency of 100% was obtained. The second simulation considered that only a fraction of the oxygen carrier of $\chi_{OC,v}$ = 0.53% is in contact with the volatile matter. It turned out that the predictions obtained with the model generally agreed with the experimental results, since the resulting $\eta_{comb\ FR}$ obtained was 89.9%. In both simulations the char conversion and carbon capture efficiency simulated were close to the values obtained experimentally. Note that the introduction of $\chi_{OC,v}$ affects the combustion efficiency, being its effect on η_{CC} and X_{char} of very low relevance. In the simulation made considering $\chi_{OC,v}$=0.53%, the mass fraction of char in the fuel reactor, f_C, had a value of 0.34% and the calculated ilmenite conversion variation ΔX_s was 24.7%.

Fig. 6 represents the evolution of CH_4, H_2, CO, CO_2 and H_2O molar flows within the fuel reactor bed, expressed as mass fraction of the bed, $m_{OC}/m_{OC,tot}$, for a total solids inventory of 3100 kg/MW_{th}. Fig. 6a) shows the flows in the dense bed, that is, derived from the gasification; Fig. 6b) represents the evolution of the volatile matter species released in the plume; and the total sum of the flows of both phases is shown in Fig. 6c).

In the dense bed all the gasification products, i.e., H_2 and CO, are fully oxidized by the oxygen carrier and the dense bed is only composed by increasing CO_2 from char oxidation and the H_2O as gasification agent. In the plume both CH_4 and H_2 decrease with the reactor mass. CH_4 comes only as part of the released volatile matter species and it is gradually consumed by its oxidation with the oxygen carrier. H_2 and CO come from volatile matter release and as intermediates of CH_4 oxidation. H_2 disappears continuously along the bed mass as it is quickly oxidized by ilmenite, while the CO profile has a maximum because there is competition between the CO generation and its reaction with the oxygen carrier.

After seeing that the model predicts the experimental results with a determined $\chi_{OC,v}$, simulation and process optimization proceed and thereby solutions for the modeling and scale-up to a pilot plant or an industrial power plant can be performed. The effect of the main variables in CLC with solid fuels is analyzed. In each evaluated case, the solids inventory was taken as independent variable.

4.2. Influence of the fuel reactor temperature

Temperature was evaluated as one of the main operating variables in a CLC system [5,19,28]. These and all the following simulations were done using fresh El Cerrejón coal as fuel. Fig. 7 shows the obtained η_{CC}, X_{char} and $\eta_{comb\ FR}$ with increasing solids inventory in the fuel reactor for fuel reactor temperatures of 900, 950 and 1000ºC and considering a system without carbon separation system. Gasification and combustion reactions are promoted with the temperature, and thus X_{char}, η_{CC} and $\eta_{comb\ FR}$, increased at higher temperatures. This was also seen experimentally by Cuadrat et al. with El Cerrejón coal [5] and Berguerand et al. [28] with pet coke.

It is clear that the fuel reactor needs to have enough oxygen carrier inventory to oxidize the fuel and to enhance the extent of gasification, since the residence time increases. Besides, the presence of an oxygen carrier increases the gasification rate because the CO and H_2 concentrations decrease and thus their inhibitory effect, as it has been experimentally tested [7,15]. For all the temperatures simulated and up to a solids inventory of 2000 kg/MW_{th} all efficiencies increase substantially. For higher inventories the beneficial effect is not so intense. With an inventory of 2000 kg/MW_{th}, $\eta_{comb\ FR}$ is 89% and it increases up to 98.7% with 5000 kg/MW_{th}, so it is not worth it to increase so much the solids inventory, as well as the size and investment of such big facility. At

950ºC as reference temperature, and with an inventory of 2000 kg/MW_{th}, values obtained for char conversion and carbon capture efficiency were X_{char} = 33.4% and η_{CC} = 52.5%. However, not even with an inventory of 10000 kg/MW_{th} full carbon capture could be obtained.

In order to get higher extent of gasification, it was proposed to separate the char that has not been gasified and recirculate it back to the fuel reactor, in order to increase the residence time of char particles and thereby raise the carbon capture efficiency. This can be made by means of a carbon stripper, whose beneficial effect has been experimentally confirmed [8]. The critical role of the carbon stripper has been pointed out in various previous studies [18,29]. Thus, the subsequent studies of the influence of several parameters are done considering that the iG-CLC system accounts with a carbon separation system.

Fig. 8 shows the concentrations of H_2, CO and CH_4 at the fuel reactor outlet when changing the fuel reactor temperature for increasing solids inventory in an iG-CLC system with a carbon stripper of 90% efficiency. 90% can be considered as a very high and extreme value of efficiency for a carbon separation system, but in this study it is taken to assess how much the CLC performance can be improved with such a good separation system and better see the influence of other parameters if carbon was highly separated and recirculated. The simulated outgoing unburnt H_2, CO and CH_4 decrease as the temperature rises because both gasification and oxidation reactions are faster. For inventories lower than 1000 kg/MW_{th}, the CO concentration at higher temperatures is higher. This is attributed to a more important improvement in the gasification rate and reaction of CH_4 –as CO is an intermediate product of CH_4 oxidation–, compared to the increase in the oxidation rate of CO.

Fig. 9 represents the carbon capture and char conversion in the process, where it can be seen that to get high performance of the process, an inventory between 1000 and 2000 kg/MW_{th} seem to be necessary and reasonable at all temperatures tested. To get high gasification and oxidation rates, it is necessary to work at high temperatures. As an example, with an inventory of 2000 kg/MW_{th} and η_{CS} = 90%, predictions of η_{CC} of 79.3% at 900ºC and 90.7% at 1000ºC were obtained. Note the important increase in the carbon capture and the char conversion when using the carbon separation system. All the values of η_{CC} obtained with η_{CS} = 0%, i.e. for a system with no carbon separation

system, were lower. Therefore, the presence of a carbon stripper is confirmed to be fundamental in order to increase the coal fed into the fuel reactor.

The simulated performance of the process regarding the oxidation of volatiles and gasification products is shown in Fig. 10. In Fig. 10a) it can be seen that the fuel reactor combustion efficiency grows with the temperature because of the increase in the oxidation reaction of ilmenite with the products of gasification and devolatilization. Above 900ºC, the minimum solids inventory needed to obtain $\eta_{comb\ FR}$ above 85% is 1000 kg/MW_{th}. As an example, with a solids inventory of 2000 kg/MW_{th}, the simulated resulting $\eta_{comb\ FR}$ was 86.0% at 900ºC, 90.7% at 950ºC and 94.2% at 1000ºC. As there is some H_2, CO and CH_4 at the fuel reactor outlet, there must be a subsequent oxidation step to fully burn the fuel reactor stream. Fig. 10b) plots the simulated total oxygen demand, defined as the fraction of the oxygen demanded by the coal fed that is necessary to burn the fuel reactor outlet gases to CO_2 and H_2O. This is the oxygen that should be supplied in a later polishing step to ensure final full combustion of the fuel. The oxygen demand in the polishing step decreases with an increase of the fuel reactor temperature. It is rather high at low inventories and decreases a lot at higher inventories up to 2000 kg/MW_{th}. For instance with an inventory of 2000 kg/MW_{th} the total oxygen demand is 5.3% at 1000ºC. For an optimum performance of the iG-CLC system, it would be best to operate at temperatures above 950ºC.

4.3. Influence of carbon stripper efficiency, η_{CS}

Fig. 11 shows the concentrations of H_2, CO and CH_4 at the fuel reactor outlet predicted with increasing solids inventory for η_{CS} = 0%, 80%, 90% and 100% at a fuel reactor temperature of 950ºC. As expected, for all η_{CS} tested, for higher solids inventories, the amount of released gaseous fuels that are not fully burnt is lower, i.e., H_2, CO and CH_4 mainly because the corresponding increase in the residence time of char particles in the reactor. In a lower relevance, there is more oxygen carrier available to react and its average reactivity is slightly higher. In all cases this improvement in the oxidation and the corresponding decrease in the H_2, CO and CH_4 concentrations is sharper from inventories up to 2000 kg/MW_{th}.

H_2 and CH_4 concentrations at the fuel reactor outlet decrease somewhat when η_{CS} increases. That is because more gasification products are being generated and as they are better oxidized, more CO_2 and H_2O are generated and the concentration of the

unburnt gaseous species decrease. The combustion of the gasification products is better because they are generated in the dense bed of the fluidized-bed and they get in more intimate contact with the oxygen carrier particles, whereas the bubbles of volatile matter formed have worse contact with the oxygen carrier. The concentration of CO at the fuel reactor outlet has maximum values for inventories of around 500 kg/MW_{th} with η_{CS} = 0% to 90%. Char recirculation causes an increase of char concentration in the bed. Thus, the increase in the CO generation rate from gasification leads to those maximum values. Compared with other values of η_{CS}, in case of having a carbon separation system with 100% efficiency, the CO concentration is higher for low inventories, as there is a lot of CO being generated from char gasification, which ilmenite is less effective to convert to CO_2 when the solids inventory is lower than 400 kg/MW_{th}.

Fig. 12 shows the simulated char conversion, carbon capture and combustion efficiencies with a wide range of oxygen carrier inventory if the system has a carbon stripper of efficiency 0%, 80%, 90% and 100%. Higher η_{CS} leads to higher η_{CC}, which is essential in this process. For example, with 1000 kg/MW_{th} at 950ºC the resulting simulated η_{CC} increase from 45.2% with η_{CS} = 0% to 79.8% with η_{CS} = 90%. That is, this process needs a char recirculation system to achieve satisfactory values of η_{CC}. Obviously, η_{CS} = 100% means that both char conversion and carbon capture efficiencies are 100%, since there is no char transferred to the air reactor. The char concentration in the bed is increased with the carbon stripper efficiency: with 1000 kg/MW_{th} at 950ºC f_C was 0.36% with η_{CS} = 0% and raised to 1.32% with η_{CS} = 90%. This fact was advanced in a theoretical analysis of the results obtained in a batch fluidized bed reactor [7].

As it could be foreseen from the outlet concentrations, the process performance for all η_{CS} simulated has the higher differences and improvements up to oxygen carrier inventories of 1000-2000 kg/MW_{th}. Furthermore, from an inventory of 2000 kg/MW_{th} an increase in η_{CS} scarcely influences the combustion efficiency. For adequate values of inventory and with the presence of a carbon separation system, there are still some unburnt gases at the fuel reactor outlet. Cuadrat et al. [5] saw experimentally that the unburnt species come from released volatile matter because they leave the bed reactor with insufficient contact with the oxygen carrier. That is, although the operation was done at high temperature, with high oxygen carrier inventory and high η_{CS}, there would be still some unburnt volatile matter and a subsequent oxygen polishing step would be necessary to fully oxidize the unburnt gases in the outlet stream from the fuel reactor.

4.4. Influence of the steam to fixed carbon ratio, H_2O/C

The motivation of evaluating the influence of steam to fixed carbon ratio, here represented as H_2O/C, is to assess if the requirements of steam as fluidizing and gasification agent are enough for the process. A ratio equal to 1 means that the amount of steam introduced is the stoichiometric flow to gasify all the carbon in char from coal fed. Fig. 13 shows predicted char conversion, carbon capture and combustion efficiency variation obtained with increasing oxygen carrier inventories with this simplified model for different H_2O/C ratios from 0.4 to 4. The calculations are made for a wide range of inventories. Possible changes in the fluid dynamics of the system derived from varying the fluidization velocity are not taken into account in the results presented here.

It can be seen that this ratio has negligible influence on the combustion efficiency. On the other hand, higher H_2O/C ratio leads to enhanced char conversion and thus carbon capture efficiency. However the effect is of low relevance for $H_2O/C > 0.7$ and no further improvement for ratios above 2 was found. The reason for this is that H_2O is only an intermediate compound in coal conversion, i.e. H_2O is consumed by char gasification but is regenerated by oxidation of H_2 produced during gasification. Both reactions happen inside the fuel reactor.

Although a H_2O/C ratio of 0.4 could be insufficient to ensure high gasification extent, with a H_2O/C ratio of 0.7 similar X_{char} values to the maximum are obtained. Thus, the ratio H_2O/C has very little influence on the process performance and it seems reasonable to work with a H_2O/C ratio of 0.7, as high values of η_{CC} would be obtained and some additional energy for steam evaporation would be saved. The same gasification promotion trends and the independence of the oxidation reaction when increasing the H_2O/C ratio was experimentally seen in tests in a continuous 500 W_{th} CLC facility that used this type of fuel and ilmenite as oxygen carrier [12].

4.5. Influence of the gasification agent type: H_2O:CO_2 mixtures

The motivation of using CO_2 is that CO_2 is a gasification agent and that the recirculation of part of the fuel reactor outlet stream will lead to savings of energy that are needed for steam generation and therefore increase the efficiency of the whole process. Fig. 14 shows that the carbon capture and char gasification extent increase when there is higher steam fraction in the gasification agent, being this less noticeable for higher η_{CS}. This is

because for this fuel the gasification rate by steam is faster than gasification by CO_2, as it was assessed during kinetics determination. However, the influence of the type of gasification agent in the combustion efficiency is not very relevant. Although steam gasification generates H_2 which is faster oxidized by ilmenite than CO, the reaction rate of ilmenite with the gases generated is faster than their generation rate. Thus, the slight increase in $\eta_{comb\ FR}$ with higher H_2O fraction that can be seen in Fig. 14c) can be only partially explained by the enhanced gasification. The generation of a higher flow of gasification products -which are better burnt because they have better contact with the oxygen carrier- leads to higher combustion efficiency of the gases in the fuel reactor. To maintain high gasification rates a carbon separation system should be implemented and some CO_2 could be recirculated, finding a balance between the increase in the energy efficiency of the whole system and the decrease in the carbon capture. For higher efficiencies of the carbon separation system, the influence of the type of gasification agent and the corresponding gasification rate are lower. Nevertheless, the char concentration in the fuel reactor bed increases as the char gasification rate decreases, as it is the case of using more CO_2 in the gas mixture. This fact will affect the design of the carbon separation system, because the load of char will be higher if CO_2 is used as gasification agent.

4.6. Influence of the oxygen carrier to fuel ratio, ϕ

One important variable in the CLC process is the oxygen carrier to fuel ratio, ϕ. This ratio indicates the oxygen that can be supplied by the circulating ilmenite compared to the oxygen needed to burn the fuel fed. In stoichiometric conditions the ϕ ratio is equal to one. Fig. 15 shows the carbon capture and combustion efficiencies for increasing fuel reactor inventories and for oxygen carrier to fuel ratios from 1.1 to 3.3.

The carbon capture efficiency clearly decreases for higher ϕ. High oxygen carrier to fuel ratio means high solids recirculation rate and thereby low residence time. The lower residence time leads to lower extent of gasification and thereby lower η_{CC}. Moreover, and increase in the solids circulation rate entails a decrease in the char concentration in the bed. For higher solids recirculation rates and higher ϕ, f_C decreases correspondingly: with 1000 kg/MW_{th} at 950ºC f_C was 1.70% with ϕ = 1.1 and decreased to 1.05% with ϕ = 3.3.

Fig. 16 plots the resulting combustion efficiency with increasing ϕ for set inventories from 200 to 5000 kg/MW_{th}. Complementary to Fig. 15b), it shows that for high inventories the combustion efficiency increases for higher ϕ because higher amount of oxygen carrier is recirculated between reactors. When more ilmenite is recirculated, it is less converted. Thus, the oxygen carrier average reactivity is higher and it is more capable to convert faster the released gaseous fuels. On the other hand, for inventories below 500 kg/MW_{th} $\eta_{comb\ FR}$ has a slight decrease with increasing ϕ because there is competition between the lower average reactivity and oxygen availability with the higher generation of gasification products which are better oxidized. The trend of increasing $\eta_{comb\ FR}$ for higher ϕ was experimentally seen for gaseous fuels [30,31]. The increase of char conversion and carbon capture efficiency and decrease of $\eta_{comb\ FR}$ with rising ϕ were observed with this type of fuel and oxygen carrier by Cuadrat et al. during CLC fuelled with coal in a continuous unit [12].

The negative influence of the gasification step as ϕ increases has higher relevance as η_{CS} decreases. However, $\eta_{comb\ FR}$ in CLC with solid fuels, as well as with gaseous fuels, would increase with the oxygen carrier to fuel ratio if high η_{CC} were reached, that is, when the gasification step did not influence the system performance.

4.7. Influence of the reduction degree of the oxygen carrier, $X_{s,in}$

The reduction degree of the oxygen carrier at the air reactor outlet, $X_{s,in}$, establishes that the minimum stoichiometric oxygen carrier to fuel ratio is $1/X_{s,in}$. It also determines the oxygen carrier average reactivity. For the fuel reactor, when the oxygen carrier is more oxidized, the average reactivity and the combustion efficiency are higher. However, when the need of reoxidation is higher, the inventory needed in the air reactor is greater. The optimum value that minimizes the total inventory in both reactors is therefore an intermediate conversion that depends on the reduction and oxidation kinetics [27]. As a reference default value, the previous simulations have been performed with an oxygen carrier reduction degree in the air reactor $X_{s,in}$ of 0. Fig. 17 represents the combustion efficiency variation for increasing $X_{s,in}$ when ϕ = 2. From 0 and up to $X_{s,in}$=0.4, $\eta_{comb\ FR}$ is scarcely influenced. From 0.4 the average reactivity decreases too much. The theoretical minimum value for $X_{s,in}$ is 0.5 when ϕ = 2 in order to transport the required oxygen from the air reactor to full oxidize the fuel fed. However, since the resulting η_{CC} is lower than 100%, for this simulation $X_{s,in}$ could be decreased to 0.7 to have enough

oxygen in the recirculated ilmenite to burn the carbon that is converted in the fuel reactor. However, in that case the resulting $\eta_{comb\ FR}$ was only 60%. Thus, as first approach and without a more complete study that included the air reactor, it can be assumed that the optimum $X_{s,in}$ is within the range 0-0.4.

4.8. Influence of increasing the oxygen carrier reaction rate

An appropriate oxygen carrier in a CLC process should have enough reactivity with the fuel. In CLC with gaseous fuels higher oxygen carrier reactivity leads directly to an improvement of the process efficiency for the same inventory and it will be able to work with lower inventories. In case of CLC with solid fuels, another factor must be taken into account, which is the gasification, as it is the limiting step of this process. Fig. 18 shows the resulting carbon capture, char conversion and combustion efficiencies predicted when increasing the oxygen carrier reaction rates. In these simulations, reaction rate of ilmenite with all the gases -that is, H_2, CO and CH_4- is considered to be multiplied by a factor represented by $(-r)/(-r_{ilm})$, being $(-r_{ilm})$ the ilmenite reaction rate. The results show that although the final combustion efficiency increases with an enhancement in the oxygen carrier reaction rate, the influence on both char conversion and carbon capture efficiency is negligible. This has been calculated for a system without carbon separation system and considering that the process accounts with a carbon stripper with 90% efficiency. Thus, the use of an oxygen carrier with high reactivity is important in order to reach high combustion efficiencies in the fuel reactor, but is not the key factor in iG-CLC to get high η_{CC}.

4.9. Improvement of the volatile matter oxidation

The volatile matter is released in a plume and the fraction of the oxygen carrier which is in contact with the volatile matter resulted to be quite small. Thus, there are a poor contact between volatiles and oxygen carrier particles which led to low value of the combustion efficiency. However, note that the bed is a bubbling fluidized bed and the height in the simulated facility is only 20 cm. The contact efficiency of volatiles with solid particles can be improved in larger circulating fluidized beds. Besides, the contact of volatile matter with the oxygen carrier in a fluidized bed combustor could be improved by enhancing their dispersion along the bed surface, as by means of an increase of the coal feeding points [32]. Any change in the contact efficiency of

volatiles can be simulated by the model by varying the parameter $\chi_{OC,v}$. Fig. 19 shows the effect of $\chi_{OC,v}$ on the combustion efficiency for different oxygen carrier inventories in the fuel reactor. The char conversion and carbon capture for this case are not affected, as the combustion efficiency lower than 1 was due to unburnt volatile matter and the gasification products were completely oxidized in all cases. So it was not possible to improve the char conversion due to decrease in the gasification inhibition. The $\chi_{OC,v}$ obtained from experimental results in the continuous unit was 0.53%. As can be observed there is a big effect of $\chi_{OC,v}$ on the combustion efficiency and $\eta_{comb\ FR}$ can be increased from 80.8% to 99% if $\chi_{OC,v}$ increased from 0.53% to 3% with an inventory of 1000 kg/MW_{th}.

A second option to fully burn the volatile matter is to implement a second step in the fuel reactor (FR2), whose fuel would be the outlet gaseous stream of the solid fuelled fuel reactor (FR1). The idea of installing a second stage for the complete combustion of volatiles was first brought up by Lewis and Gilliland [33]. It is also an alternative to the oxygen polishing step. As the fuel is gaseous, this second reactor would not be limited by the gasification step and the contact with the oxygen carrier would be much better, since the fuel would be introduced at the bottom of the reactor and not released in a plume. Fig. 20 shows the minimum ilmenite inventory that would be required in the second fuel reactor step to fully burn the outlet stream coming from the first fuel reactor for different inventories in the first fuel reactor, for the case of using a carbon separation system with 90% efficiency and working at 950ºC. In FR2 it is considered that the whole oxygen carrier bed is in contact with both volatiles and gasification products.

Values obtained for the second step fuel reactor are small: the maximum is 45 kg/MW_{th}. Note that although for increasing inventory in FR1, the quantities of unconverted gases are lower, but they are more diluted because the total flows are higher as more H_2O and CO_2 are generated. This trade-off between the dilution and the amount of gaseous fuels introduced in the second reactor explains the first increase in the resulting inventory needed for the second fuel reactor.

This seems a very promising option, as with an inventory of 1000 kg/MW_{th} in the first fuel reactor, only additional 44 kg/MW_{th} in the second step of the fuel reactor FR2 would be needed to fully oxidize the fuel. For 2000 kg/MW_{th} in FR1, the second fuel reactor would need 40 kg/MW_{th}. It is necessary to have an efficient carbon separation system, as well as to have enough inventory in the first step of the fuel reactor to

achieve high carbon capture and combustion efficiency. However, the inventory of the first step of the fuel reactor could be decreased as the outlet gases can be completely burnt in the second fuel reactor, which is much smaller.

5. Conclusions

In this work a simplified model for in situ gasification Chemical-Looping Combustion (iG-CLC) with solid fuels has been developed, based on the differential mass balances with reaction of the fuel reactor for the gasification products evolved in the dense bed and volatile matter in form of a plume. The model includes the kinetics of coal char gasification and reaction of gasification and devolatilization products with the oxygen carrier. The model results were compared with experimental results from tests performed in a 500W_{th} facility fuelled with "El Cerrejón" bituminous coal and ilmenite as oxygen carrier. The limitation to obtain full combustion in the fuel reactor was assigned to poor contact of the volatile matter with the oxygen carrier. A division of the oxygen carrier bed in the fuel reactor was done and it was calculated that the fraction of oxygen carrier in contact with the volatiles was 0.53% for the simulated facility. After that, the operating conditions for iG-CLC were optimized by analyzing the effect of relevant operating conditions on the performance of the system.

It was seen that it is essential that the fuel reactor has enough inventory to oxidize the fuel and to enhance the extent of carbon capture, since the residence time increases. The carbon capture was directly related to the extent of gasification, which is promoted by increasing the temperature or the residence time of char particles in the fuel reactor. It is highly beneficial to increase the solids inventory up to 1000 kg/MW_{th}, but further increase does not give a relevant improvement in the carbon capture. With inventory in the fuel reactor of 1000 kg/MW_{th}, at 1000ºC and an efficiency of the carbon separation system of 90%, the carbon capture obtained is 86.0%. To further enhance the carbon capture, to increase the efficiency of the carbon separation system is preferred rather than increasing the solids inventory.

As there is some H_2, CO and CH_4 at the fuel reactor outlet, there must be a subsequent oxidation step to fully burn the fuel reactor stream. The corresponding calculated oxygen demand of this subsequent oxygen polishing step was 5.3% at 1000ºC.

High oxygen carrier to fuel ratio means high solids recirculation rate and thereby lower residence time, which leads a decrease in carbon capture efficiency. The negative

influence of the gasification step as the oxygen carrier to fuel ratio increases had lower relevance as the efficiency of the carbon separation system increased.

To have a high reactive oxygen carrier is important to reach high combustion efficiencies, but is not the key factor to get high performance of the process. Lower influence on the iG-CLC performance was observed for the gasification agent to fixed carbon ratio; the type of gasification agent in case of different H_2O:CO_2 mixtures, being the influence of the gasification agent type of less importance for higher efficiencies of the carbon separation system; and the reduction degree of the oxygen carrier in the air reactor outlet.

Improvement in the contact of the volatile matter with the oxygen carrier is necessary to get high combustion efficiency. Some design solutions can be applied to increase the contact. An improvement in the volatile matter dispersion along the bed would increase the contact efficiency of volatiles. Full combustion can be also reached by implementing a second fuel reactor step, whose fuel would be the outlet gaseous stream of the first fuel reactor. The inventories needed in this second fuel reactor are very small: 45 kg/MW_{th} as maximum value.

The simulation of a wide range of conditions showed that an optimized iG-CLC system for solid fuels with ilmenite as oxygen carrier should have a carbon separation system with high efficiency above 90% and the fuel reactor temperature should be above 950ºC. A gasification agent to fixed carbon ratio of 0.7 would be enough and some CO_2 from the outlet fuel reactor could be recirculated and used as gasification agent. The optimum reduction degree in the air reactor outlet would be within the range 0-0.4. The contact of the volatile matter with the oxygen carrier should be improved with some design solutions or the implementation of a second fuel reactor is proposed as a very promising option to fully burn the volatile matter and besides avoid another oxygen polishing step. With these measures and range of values of the parameters and with an inventory around 1000 kg/MW_{th}, carbon capture efficiency higher than 90% and full combustion will be reached.

Notation

$\bar{b}$ = average stoichiometric coefficient for reaction of solid with reacting gas

$[C]_{fuel}$, $[H]_{fuel}$, $[O]_{fuel}$ fraction of carbon, hydrogen and oxygen, respectively, in the fuel

C_g = reacting gas concentration (mol/m^3)

CLC Chemical Looping Combustion

d = stoichiometric factor in the fuel combustion reaction with oxygen (mol O_2 per mol of fuel)

E_a activation energy (kJ/mol)

f_C carbon concentration in the fuel reactor bed

$F_{C,char}$ carbon flow from the char introduced with the fuel (mol/s)

$(F_{C,char})_{in}$ carbon flow from char entering the fuel reactor (mol/s)

$(F_{C,char})_{out}$ carbon flow of ungasified char that exits the fuel reactor (mol/s)

$(F_C)_{gp}$ flow of carbon contained in the products of char gasification (mol/s)

$(F_C)_{vol}$ flow of carbon contained in the volatile matter (mol/s)

$(F_{CO_2})_{in}$ flow of introduced CO_2 as gasification agent (mol/s)

$F_{CO_2,AR}$ molar flow of carbon that is oxidized in the air reactor (mol/s)

$F_{i,e,1}$, $F_{i,e,2}$ gas flows of the gasification product i in the dense bed at the inlet and outlet of an inventory differential mass (mol/s)

$F_{i,v,1}$, $F_{i,v,2}$ gas flows of the released gas i in the volatiles at the inlet and outlet of an inventory differential mass (mol/s)

F_j flow of the gas component j in the dense bed (mol/s)

F_k flow of the gas component k in the plume (mol/s)

F_{H_2}, F_{CO}, F_{CH_4}, F_{CO_2}, F_{H_2O} molar flows of H_2, CO, CH_4, CO_2 and H_2O, respectively

$F^0_{k,vol}$ flow of the gas component k that is released when coal is devolatilized (mol/s)

$F^0_{j,gas}$ flow of gas j introduced as gasification agent (mol/s)

FR1 solid fuelled fuel reactor

FR2 second fuel reactor proposed

G_S solids circulation rate (kg/s)

H_2O/C gasification agent to fixed carbon ratio

iG-CLC in situ Gasification-Chemical Looping Combustion

k_1, k_2 kinetic constants in the gasification rate ($s^{-1}bar^{-1}$)

k_3 kinetic constants in the gasification rate (s^{-1})

k_{s0} = pre-exponential factor for chemical kinetic constant ($mol^{1-n}\ m^{3n-2}\ s^{-1}$)

Me_xO_y oxygen carrier in its oxidized form

Me_xO_{y-1} oxygen carrier in its reduced form

$\dot{m}_{fuel,in}$ coal feeding flow (kg/s)

M_C molecular weight of carbon (kg/mol)

M_O molecular weight of oxygen (kg/mol)

$\dot{m}_{OC}$ solids circulation rate per MW_{th} of fuel (kg/s per MW_{th})

m_{OC} solids inventory (kg per MW_{th})

n reaction order

p_{prod} partial pressure of the gasification products (bar)

p_{react} partial pressure of the gaseous reactants (bar)

$(-r_{ilm,i})$ reaction rate of ilmenite for a given reaction i (s^{-1})

(-r) oxygen carrier reaction rate (s^{-1})

($-r_{ilm}$) ilmenite reaction rate (s^{-1})

r_{gasif} gasification rate (s^{-1})

$(r_{gasif})_{H_2O}$, $(r_{gasif})_{CO_2}$ char gasification rates with H_2O and CO_2, respectively (s^{-1})

$(-r_{ilm,H_2})$, $(-r_{ilm,CO})$, $(-r_{ilm,CH_4})$ reaction rates of ilmenite with H_2, CO and CH_4, respectively (s^{-1})

r_{grain} grain radius (m)

$R_{O,ilm}$ oxygen transport capacity of ilmenite (kg oxygen/kg oxygen carrier)

t time (s)

T_{FR} fuel reactor temperature (ºC)

X_{char} char conversion

$X_{s,i}$ conversion of the oxygen carrier of reaction i

$X_{s,in}$ conversion of solids at the fuel reactor inlet

ΔX_s variation of the solids conversion in the reactor

Φ characteristic reactivity of the oxygen carrier

Ω_T oxygen demand (%)

Ω_{coal} oxygen demanded by the coal feeding flow (mol O/s)

ϕ oxygen carrier to fuel ratio

η_{CC} carbon capture efficiency

η_{CS} carbon stripper efficiency

$\eta_{comb\ FR}$ fuel reactor combustion efficiency

$\chi_{OC,v}$ fraction of oxygen carrier in bed that is in contact with the volatile matter

ρ_m= molar density (mol/m^3)

τ time for complete solid conversion of the oxygen carrier for the reduction reaction considered (s)

Acknowledgments

This work was partially supported by the Spanish Ministry of Science and Innovation (Project ENE2010-19550). A. Cuadrat thanks CSIC for the JAE Pre. fellowship. Alberto Abad thanks to the Ministerio de Ciencia e Innovación for the financial support in the course of the I3 Program.

References

[1] Kerr HR. Capture and separation technology gaps and priority research needs. In: Thomas DC, Benson SM, editors. Carbon dioxide capture for storage in deep geologic formations– Results from the CO2 capture project, Oxford, UK: Elsevier; 2005, vol. 1, Chapter 38.

[2] Thambimuthu K, Soltanieh M, Abanades JC. Capture of CO2. In: Metz B, Davidson O, de Coninck HC, Loos M, Meyer LA, editors. IPCC special report on carbon dioxide capture and storage, Cambridge. UK: Cambridge University Press; 2005, chapter 3.

[3] Adánez J, Abad A, Garcia-Labiano F, Gayán P, de Diego LF. Progress in Chemical-Looping Combustion and Reforming technologies. Progress Energy Combustion Science 2012;38:215-282.

[4] Cao Y, Pan WP. Investigation of chemical looping combustion by solid fuels. 1. Process analysis. Energy & Fuels 2006;20:1836-1844.

[5] Cuadrat A, Abad A, García-Labiano F, Gayán P, de Diego LF, Adánez J. The use of ilmenite as oxygen carrier in a 500 Wth Chemical Looping Coal Combustion unit. Int J Greenhouse Gas Control 2011;5:1630–42.

[6] Berguerand N, Lyngfelt A. Design and operation of a 10 kWth chemical-looping combustor for solid fuels – Testing with South African coal. Fuel 2008;87:2713-2726.

[7] Cuadrat A, Abad A, de Diego LF, García-Labiano F, Gayán P , Adánez J. Prompt Considerations on the Design of Chemical-Looping Combustion of Coal from Experimental Tests. Fuel 2012; in press.

[8] Berguerand N, Lyngfelt A. The use of petroleum coke as fuel in a 10 kW chemical looping combustor. Int J Greenhouse Gas Control 2008;2:169-79.

[9] Leion H, Mattissson T, Lyngfelt A. Use of ores and industrial products as oxygen carriers in chemical-looping combustion. Energy Fuels 2009;23:2307-15.

[10] Leion H, Jerndal E, Steenari BM, Hermansson S, Israelsson M, Jansson E, Johnsson M, Thunberg R, Vadenbo A, Mattisson T, Lyngfelt A. Solid fuels in chemical–looping combustion using oxide scale and unprocessed iron ore as oxygen carriers. Fuel 2009;88:1945-1954.

[11] Jerndal E, Leion H, Mattisson T, Lyngfelt A. Using low–cost iron–based materials as oxygen carriers for chemical–looping combustion. Oil & Gas Science and Technology 2011;66(2):235-248.

[12] Cuadrat A, Abad A, García-Labiano F, Gayán P, de Diego LF, Adánez J. Effect of operating conditions in Chemical-Looping Combustion of coal in a 500 W_{th} unit. Int J Greenhouse Gas Control 2012;6:153-163.

[13] Abad A, Adánez J, Cuadrat A, García-Labiano F, Gayán P, de Diego LF. Reaction kinetics of ilmenite for Chemical-looping Combustion. Chemical Engineering Science 2011;66(4):689-702.

[14] Adánez J, Cuadrat A, Abad A, Gayán P, de Diego LF, García-Labiano F. Ilmenite Activation during Consecutive Redox Cycles in Chemical-Looping Combustion. Energy & Fuels 2010;24:1402-1413.

[15] Leion H, Mattisson T, Lyngfelt A. Solid fuels in chemical-looping combustion. Int J Greenhouse Gas Control 2008;2:180-193.

[16] Cuadrat A, Abad A, Adánez J, de Diego LF, García-Labiano F, Gayán P. Behavior of Ilmenite as Oxygen Carrier in Chemical-Looping Combustion. Fuel Proc Tech 2012;94(1):101-112.

[17] Mahalatkar K, O'Brien T, Huckaby ED, Kuhlman J. Computational fluid dynamic simulation of the fuel reactor of a coal–fired chemical looping combustor. Proc 1st Int Conf on Chemical Looping. Lyon, France; 2010.

[18] Ströhle J, Orth M, Epple B. Simulation of the fuel reactor of a 1 MWth chemical looping plant for coal. Proc 1st Int Conf on Chemical Looping. Lyon, France; 2010.

[19] Kolbitsch P, Pröll T, Hofbauer H. Modeling of a 120 kW chemical looping combustion reactor system using a Ni-based oxygen carrier. Chemical Engineering Science 2009;64:99-108.

[20] Brown TA, Dennis JS, Scott SA, Davidson JF, Hayhurst AN. Gasification and chemical looping combustion of a lignite char in a fluidized bed of iron oxide. Energy Fuels 2010;24:3034-48.

[21] Leion H, Mattisson T, Lyngfelt A. The use of petroleum coke as fuel in chemical looping combustion. Fuel 2007;86:1947-58.

[22] Agarwal PK, Genetti WA, Lee YY. Model for devolatilization of coal particles in fluidized beds. Fuel 1984; 63; 1157–1165.

[23] Adánez J, Miranda JL, Gavilán JM. Kinetics of a lignite-char gasification by CO_2. Fuel 1985;64(6):801-804.
[24] Abad A, Mattisson T, Lyngfelt A, Johansson M. The use of iron oxide as oxygen carrier in a chemical-looping reactor. Fuel 2007;86:1021-35.
[25] Pröll T, Mayer K, Bolhàr-Nordenkampf J, Kolbitsch P, Mattisson T, Lyngfelt A, Hofbauer H. Natural minerals as oxygen carriers for chemical looping combustion in a dual circulating fluidized bed system. Energy Procedia 2009;1:27-34.
[26] Abad A, Adánez J, García-Labiano F, de Diego LF, Gayán P. Modeling of the chemical-looping combustion of methane using a Cu-based oxygen carrier. Combustion and Flame 2010;157(3):602-615.
[27] Abad A, Adánez J, García-Labiano F, de Diego LF, Gayán P, Celaya J. Mapping of the range of operational conditions for Cu-, Fe-, and Ni-based oxygen carriers in chemical-looping combustion. Chemical Engineering Science 2007;62:533-549.
[28] Berguerand N, Lyngfelt A. Chemical-looping combustion of petroleum coke using ilmenite in a 10 kW_{th} unit-high-temperature operation. Energy & Fuels 2009;23(10):5257-5268.
[29] Kramp, M., Thon A, Hartge EU, Heinrich S, Werther J.. Carbon Stripping - A Critical Process Step in the Chemical Looping Combustion of Solid Fuels, in: 2nd International Conference on Energy Process Engineering (ICEPE 2). Efficient Carbon Capture for Coal Power Plants. ICEPE2. 2011. Franfurt, Germany.
[30] Dueso C, García-Labiano F, Adánez J, de Diego LF, Gayán P, Abad A. Syngas combustion in a chemical-looping combustion system using an impregnated Ni-based oxygen carrier. Fuel 2009;88:2357-2364.
[31] Forero CR, Gayán P, de Diego LF, Abad A, García-Labiano F, Adánez J. Syngas combustion in a 500 Wth chemical-looping combustion system using an impregnated Cu-based oxygen carrier. Fuel Proc Technol 2009;90:1471-1479.
[32] Park D, Levenspiel O, Fitzgerald TJ. Plume model for large particle fluidized-bed combustors. Fuel 1981;60(4):295-306.
[33] Lewis WK, Gilliland ER. Production of pure carbon dioxide. Patent US 2665971 1954.

Theoretical approach on the CLC performance with solid fuels: optimizing the solids inventory

Ana Cuadrat, Alberto Abad*, Pilar Gayán, Luis F. de Diego, Francisco García-Labiano, Juan Adánez

Tables

Table 1. Proximate and ultimate analyses and lower heating value of fresh and pre-treated El Cerrejón coal.

Table 2. Mass (g) of the different gaseous species generated from the release of the volatile matter of 100 g of El Cerrejón coal after CH_4 reforming, for different H_2O-CO_2 mixtures as gasification agent.

Table 3. Gasification kinetic constants for char from pre-treated El Cerrejón coal. Gasification agents: H_2O/H_2 and CO_2/CO.

Table 4. Main parameters for ilmenite reduction kinetics with H_2, CO and CH_4 at 950ºC. P=1atm.

Theoretical approach on the CLC performance with solid fuels: optimizing the solids inventory

Ana Cuadrat, Alberto Abad*, Pilar Gayán, Luis F. de Diego, Francisco García-Labiano, Juan Adánez

Table 1. Proximate and ultimate analyses and lower heating value of fresh and pre-treated El Cerrejón coal.

Fresh Colombian coal			
C	68.0 %	Moisture	6.2 %
H	4.2 %	Volatile matter	33.4 %
N	1.6 %	Fixed carbon	48.5 %
S	0.6 %	Ash	11.9 %
	Lower Heating Value: 25878 kJ/kg		
Pre-treated Colombian coal			
C	65.8 %	Moisture	2.3 %
H	3.3 %	Volatile matter	33.0 %
N	1.6 %	Fixed carbon	55.9 %
S	0.6 %	Ash	8.8 %
	Lower Heating Value: 21899 kJ/kg		

Table 2. Mass (g) of the different gaseous species generated from the release of the volatile matter of 100 g of El Cerrejón coal after CH_4 reforming, for different H_2O-CO_2 mixtures as gasification agent.

Gasification agent	CO	CO_2	CH_4	H_2O	H_2
100% H_2O	5.7	42.8	7.1	-27.8	5.5
50% H_2O + 50% CO_2	23.1	12.7	8.8	-14.7	3.4
100% CO_2	46.5	-29.1	9.9	4.8	1.2

Table 3. Gasification kinetic constants for char from pre-treated El Cerrejón coal. Gasification agents: H_2O/H_2 and CO_2/CO.

	H_2O			CO_2		
	$k_{1,H2O}$ ($s^{-1}bar^{-1}$)	$k_{2,H2O}$ ($s^{-1}bar^{-1}$)	$k_{3,H2O}$ (s^{-1})	$k_{1,CO2}$ ($s^{-1}bar^{-1}$)	$k_{2,CO2}$ ($s^{-1}bar^{-1}$)	$k_{3,CO2}$ (s^{-1})
k_o	52.6	$2.81 \cdot 10^{-6}$	$8.1 \cdot 10^{-9}$	$4.53 \cdot 10^{3}$	$3.28 \cdot 10^{-7}$	$1.84 \cdot 10^{-6}$
E_a (kJ/mol)	95.1	-135.1	-218.5	160.1	-158.5	-157.6

Table 4. Main parameters for ilmenite reduction kinetics with H_2, CO and CH_4 at 950ºC. P=1atm.

	H_2	CO	CH_4
d	0.5	0.5	2
ρ_m (mol/m^3)	13589	13589	13589
r_{grain} (m)	$1.25 \cdot 10^{-6}$	$1.25 \cdot 10^{-6}$	$1.25 \cdot 10^{-6}$
$\bar{b}$	1.45	1.45	1.45
k_{so}	0.062	0.1	42
E_a (kJ/mol)	65	80.7	135.9
n	1	0.8	1

Theoretical approach on the CLC performance with solid fuels: optimizing the solids inventory

Ana Cuadrat, Alberto Abad*, Pilar Gayán, Luis F. de Diego, Francisco García-Labiano, Juan Adánez

Captions of figures

Fig. 1. Reactor scheme of the CLC process using solid fuels (- - - optional stream).

Fig. 2. Mass flows changes of the gases involved in the process –products of gasification and devolatilization- for a fuel reactor differential mass inventory, dm_{OC}.

Fig. 3. Scheme of carbon flows involved in the fuel reactor and carbon separation system.

Fig. 4. Char conversion versus time curves for the gasification reactions with H_2O of El Cerrejón coal obtained by TGA a) at different temperatures: 900ºC, 950ºC, 1000ºC and 1050ºC, using 20% H_2O + 0% H_2; and b) with 40% H_2O and different H_2 fractions: 0%, 10% 20% and 30% H_2 at 1000ºC.

Fig. 5. Fuel reactor combustion efficiencies obtained experimentally and theoretically with the model, considering $\chi_{OC,v}$ = 0.53%, at different fuel reactor temperatures. Solids inventory = 3100 kg/MW_{th}. H_2O/C=0.7. ϕ=2. η_{CS}=0. $X_{s,in}$=0. Fuel: pre-treated El Cerrejón coal.

Fig. 6. Evolution of the a) in the dense bed b) in the plume and c) total CH_4, H_2, CO, CO_2 and H_2O molar flows within the fuel reactor bed, for a solids inventory of 3100 kg/MW_{th}. T_{FR}=900ºC. H_2O/C=0.7. ϕ=2. η_{CS}=0. $X_{s,in}$=0. $\chi_{OC,v}$=0.53%. Fuel: pre-treated El Cerrejón coal.

Fig. 7. Variation of a) carbon capture, b) char conversion and c) combustion efficiency with increasing solids inventory for several fuel reactor temperatures. ── 900ºC, ---- 950ºC and ····· 1000ºC. H_2O/C=0.7. ϕ=2. η_{CS}=0. $X_{s,in}$=0. $\chi_{OC,v}$=0.53%.

Fig. 8. Variation of H_2, CO and CH_4 concentrations at the fuel reactor outlet with increasing solids inventory for several fuel reactor temperatures. ── 900ºC, ---- 950ºC and ····· 1000ºC. H_2O/C=0.7. ϕ=2. η_{CS}=90%. $X_{s,in}$=0. $\chi_{OC,v}$=0.53%.

Fig. 9. Variation of a) carbon capture and b) char conversion with increasing solids inventory for several fuel reactor temperatures. ── 900ºC, ---- 950ºC and ····· 1000ºC. H_2O/C=0.7. ϕ=2. η_{CS}=90%. $X_{s,in}$=0. $\chi_{OC,v}$=0.53%.

Fig. 10. Variation of a) combustion efficiency and b) total oxygen demand with increasing solids inventory for several fuel reactor temperatures. ── 900ºC, ---- 950ºC and ····· 1000ºC. H_2O/C=0.7. ϕ=2. η_{CS}=90%. $X_{s,in}$=0. $\chi_{OC,v}$=0.53%.

Fig. 11. Variation of H_2, CO and CH_4 concentrations at the fuel reactor outlet with increasing solids inventory for η_{CS}=0%, 80%, 90% and 100%. T_{FR}=950ºC. H_2O/C=0.7. ϕ=2. $X_{s,in}$=0. $\chi_{OC,v}$=0.53%.

Fig. 12. Variation of a) carbon capture, b) char conversion and c) combustion efficiency with increasing solids inventory for η_{CS}=0, 80%, 90% and 100%. T_{FR}=950ºC. H_2O/C=0.7. ϕ=2. $X_{s,in}$=0. $\chi_{OC,v}$=0.53%.

Fig. 13. Variation of a) carbon capture, b) char conversion and c) combustion efficiencies with increasing solids inventory for H_2O/C ratios of 0.4, 0.7, 2 and 4. T_{FR}=950ºC. ϕ=2. η_{CS}=90%. $X_{s,in}$=0. $\chi_{OC,v}$=0.53%.

Fig. 14. Variation of a) carbon capture, b) char conversion and c) combustion efficiencies with different H_2O:CO_2 mixtures as gasification agent and for several η_{CS}: 0%, 80%, 90%, 95% and 98%. Inventory= 1000 kg/MW_{th}. T_{FR}=950ºC. $(H_2O+CO_2)/C$=0.7. ϕ=2. $X_{s,in}$=0. $\chi_{OC,v}$=0.53%.

Fig. 15. Variation of a) carbon capture and b) combustion efficiencies with increasing solids inventory for oxygen carrier to fuel ratios, ϕ, of 1.1, 1.2, 1.5, 2 and 3.33. T_{FR}=950ºC. H_2O/C=0.7. η_{CS}=90%. $X_{s,in}$=0. $\chi_{OC,v}$=0.53%.

Fig. 16. Resulting combustion efficiency with increasing ϕ for inventories of 200, 500, 1000 and 5000 kg/MW_{th}. T_{FR}=950ºC. H_2O/C=0.7. η_{CS}=90%. $X_{s,in}$=0. $\chi_{OC,v}$=0.53%.

Fig. 17. Combustion efficiency variation with increasing $X_{s,in}$. Inventory = 1000 kg/MW_{th}. T_{FR}=950ºC. H_2O/C=0.7. ϕ=2. η_{CS}=90%. $\chi_{OC,v}$=0.53%.

Fig. 18. Variation of a) carbon capture, b) char conversion and c) combustion efficiency with increasing oxygen carrier reaction rate, for carbon stripper efficiencies of 0% and 90%. Inventory=500 kg/MW_{th}. T_{FR}=950ºC. H_2O/C=0.7. ϕ=2. $X_{s,in}$=0.

Fig. 19. Combustion efficiency variation with increasing $\chi_{OC,v}$ for several inventories: —— 200 kg/MW_{th}, ---- 500 kg/MW_{th} and ····· 1000 kg/MW_{th}. T_{FR}=950ºC. H_2O/C=0.7. ϕ=2. η_{CS}=90%. $X_{s,in}$=0.

Fig. 20. Minimum ilmenite inventory in the second fuel reactor to completely oxidize the fuel for different inventories in the first fuel reactor. T_{FR}=950ºC. Conditions in the first fuel reactor: H_2O/C=0.7. ϕ=2. η_{CS}=90%. $X_{s,in}$=0. $\chi_{OC,v}$=0.53%.

Theoretical approach on the CLC performance with solid fuels: optimizing the solids inventory

Ana Cuadrat, Alberto Abad*, Pilar Gayán, Luis F. de Diego, Francisco García-Labiano, Juan Adánez

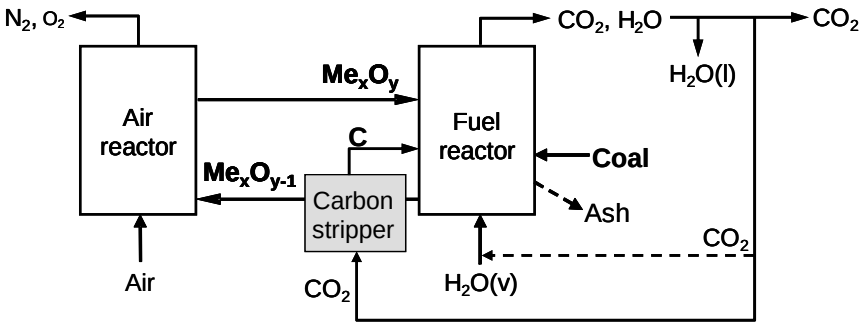

Fig. 1. Reactor scheme of the CLC process using solid fuels (- - - optional stream).

Ana Cuadrat, Alberto Abad*, Pilar Gayán, Luis F. de Diego, Francisco García-Labiano, Juan Adánez

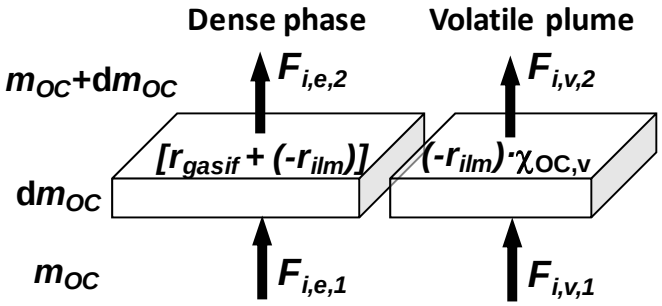

Fig. 2. Mass flows changes of the gases involved in the process –products of gasification and devolatilization- for a fuel reactor differential mass inventory, dm_{OC}.

Theoretical approach on the CLC performance with solid fuels: optimizing the solids inventory

Ana Cuadrat, Alberto Abad*, Pilar Gayán, Luis F. de Diego, Francisco García-Labiano, Juan Adánez

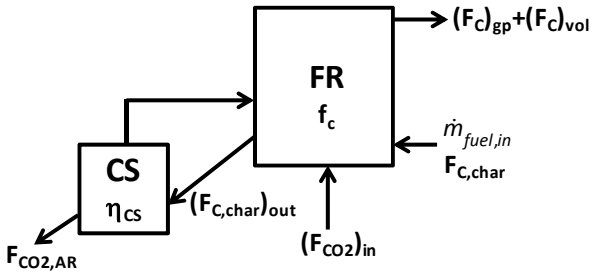

INCLUYE $(F_C)_{vol}$ en la entrada, ya que lo has puesto a la salida y queda más claro. También falta el flujo de carbono que sale del CS al FR.

Fig. 3. Scheme of carbon flows involved in the fuel reactor and carbon separation system.

Theoretical approach on the CLC performance with solid fuels: optimizing the solids inventory

Ana Cuadrat, Alberto Abad*, Pilar Gayán, Luis F. de Diego, Francisco García-Labiano, Juan Adánez

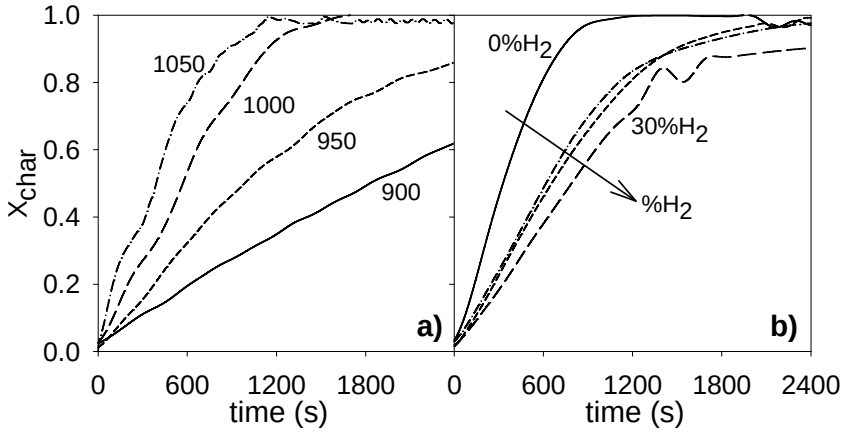

Fig. 4. Char conversion versus time curves for the gasification reactions with H_2O of El Cerrejón coal obtained by TGA a) at different temperatures: 900ºC, 950ºC, 1000ºC and 1050ºC, using 20% H_2O + 0% H_2; and b) with 40% H_2O and different H_2 fractions: 0%, 10% 20% and 30% H_2 at 1000ºC.

Theoretical approach on the CLC performance with solid fuels: optimizing the solids inventory

Ana Cuadrat, Alberto Abad*, Pilar Gayán, Luis F. de Diego, Francisco García-Labiano, Juan Adánez

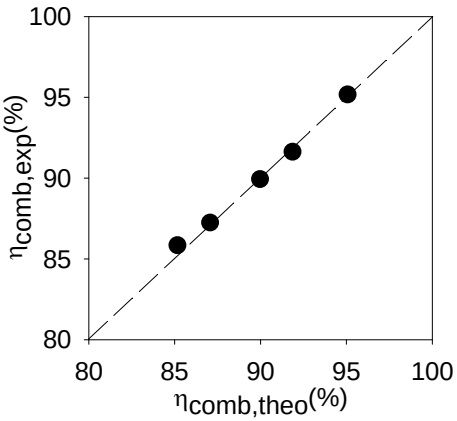

Fig. 5. Fuel reactor combustion efficiencies obtained experimentally and theoretically with the model, considering $\chi_{OC,v}$ = 0.53%, at fuel reactor temperatures in the range 880-940ºC. Solids inventory = 3100 kg/MW_{th}. H_2O/C=0.7. ϕ=2. η_{CS}=0. $X_{s,in}$= 0. Fuel: pre-treated El Cerrejón coal.

Theoretical approach on the CLC performance with solid fuels: optimizing the solids inventory

Ana Cuadrat, Alberto Abad*, Pilar Gayán, Luis F. de Diego, Francisco García-Labiano, Juan Adánez

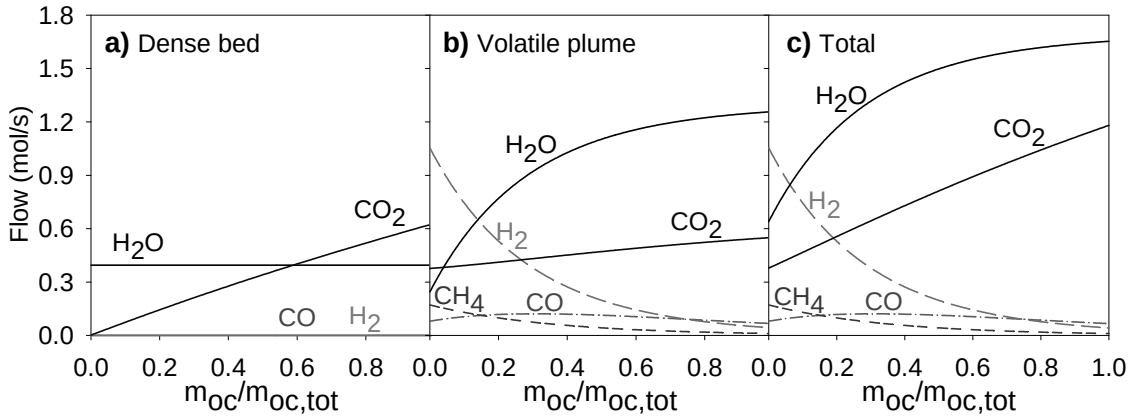

Fig. 6. Evolution of the a) in the dense bed b) in the plume and c) total CH_4, H_2, CO, CO_2 and H_2O molar flows within the fuel reactor bed, for a solids inventory of 3100 kg/MW_{th}. T_{FR}=900ºC. H_2O/C=0.7. ϕ=2. η_{CS}=0. $X_{s,in}$= 0. $\chi_{OC,v}$=0.53%. Fuel: pre-treated El Cerrejón coal.

Theoretical approach on the CLC performance with solid fuels: optimizing the solids inventory

Ana Cuadrat, Alberto Abad*, Pilar Gayán, Luis F. de Diego, Francisco García-Labiano, Juan Adánez

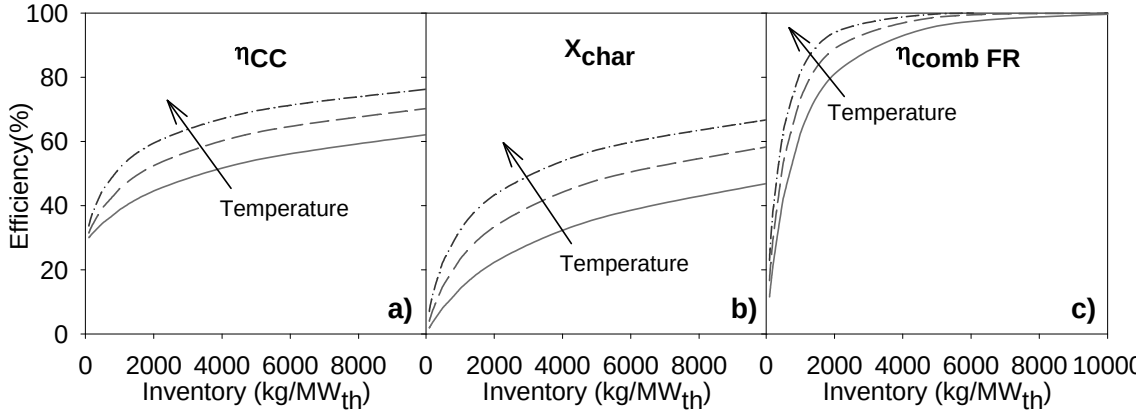

Fig. 7. Variation of a) carbon capture, b) char conversion and c) combustion efficiency with increasing solids inventory for several fuel reactor temperatures. —— 900ºC, ---- 950ºC and ····· 1000ºC. H_2O/C=0.7. ϕ=2. η_{CS}=0. $X_{s,in}$= 0. $\chi_{OC,v}$=0.53%.

Theoretical approach on the CLC performance with solid fuels: optimizing the solids inventory

Ana Cuadrat, Alberto Abad*, Pilar Gayán, Luis F. de Diego, Francisco García-Labiano, Juan Adánez

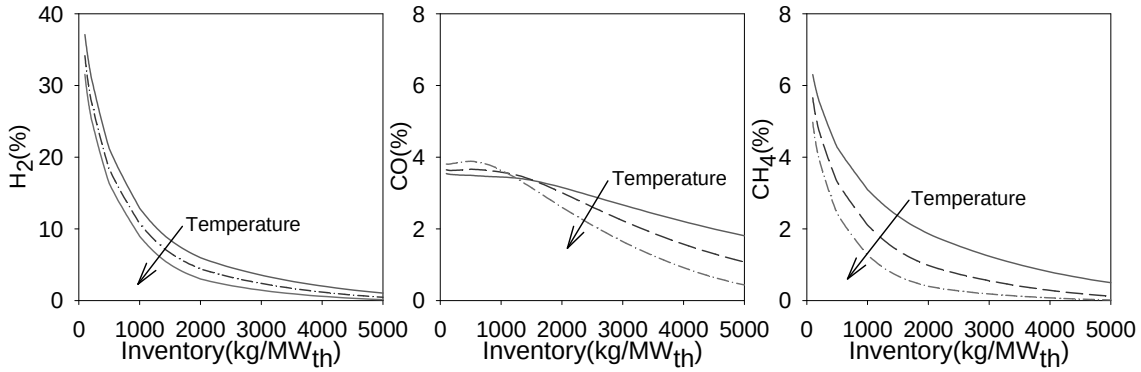

Fig. 8. Variation of H_2, CO and CH_4 concentrations at the fuel reactor outlet with increasing solids inventory for several fuel reactor temperatures. —— 900ºC, ---- 950ºC and ····· 1000ºC. $H_2O/C=0.7$. $\phi=2$. $\eta_{CS}=90\%$. $X_{s,in}= 0$. $\chi_{OC,v}=0.53\%$.

Theoretical approach on the CLC performance with solid fuels: optimizing the solids inventory

Ana Cuadrat, Alberto Abad*, Pilar Gayán, Luis F. de Diego, Francisco García-Labiano, Juan Adánez

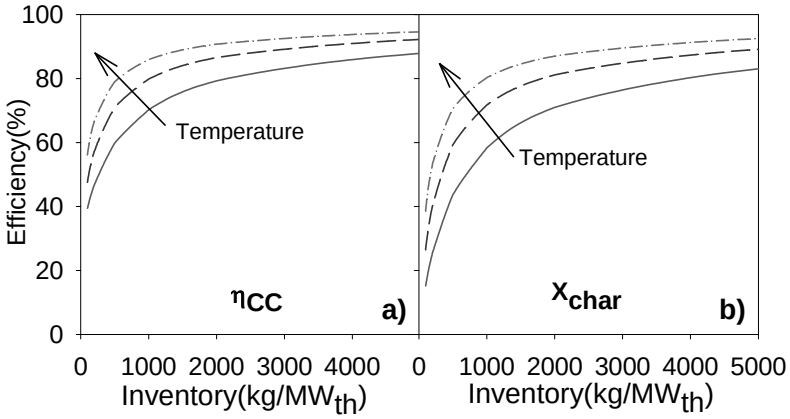

Fig. 9. Variation of a) carbon capture and b) char conversion with increasing solids inventory for several fuel reactor temperatures. —— 900ºC, ---- 950ºC and ····· 1000ºC. H_2O/C=0.7. ϕ=2. η_{CS}=90%. $X_{s,in}$= 0. $\chi_{OC,v}$=0.53%.

Theoretical approach on the CLC performance with solid fuels: optimizing the solids inventory

Ana Cuadrat, Alberto Abad*, Pilar Gayán, Luis F. de Diego, Francisco García-Labiano, Juan Adánez

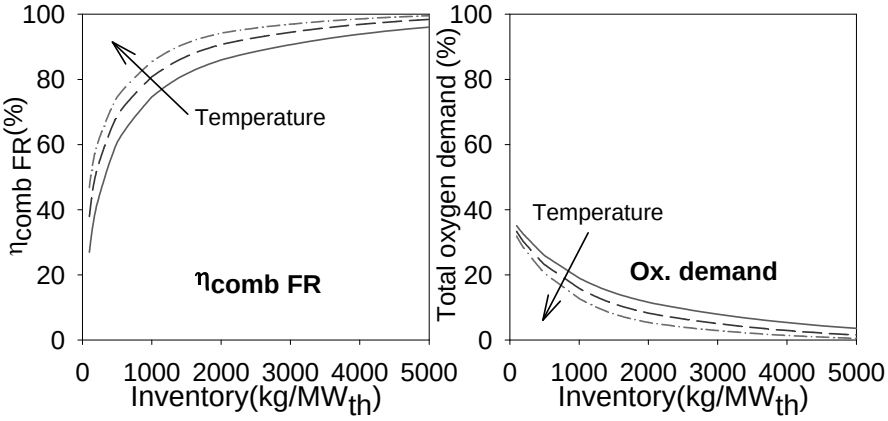

Fig. 10. Variation of a) combustion efficiency and b) total oxygen demand with increasing solids inventory for several fuel reactor temperatures. ── 900ºC, ---- 950ºC and ····· 1000ºC. H_2O/C=0.7. ϕ=2. η_{CS}=90%. $X_{s,in}$= 0. $\chi_{OC,v}$=0.53%.

Theoretical approach on the CLC performance with solid fuels: optimizing the solids inventory

Ana Cuadrat, Alberto Abad*, Pilar Gayán, Luis F. de Diego, Francisco García-Labiano, Juan Adánez

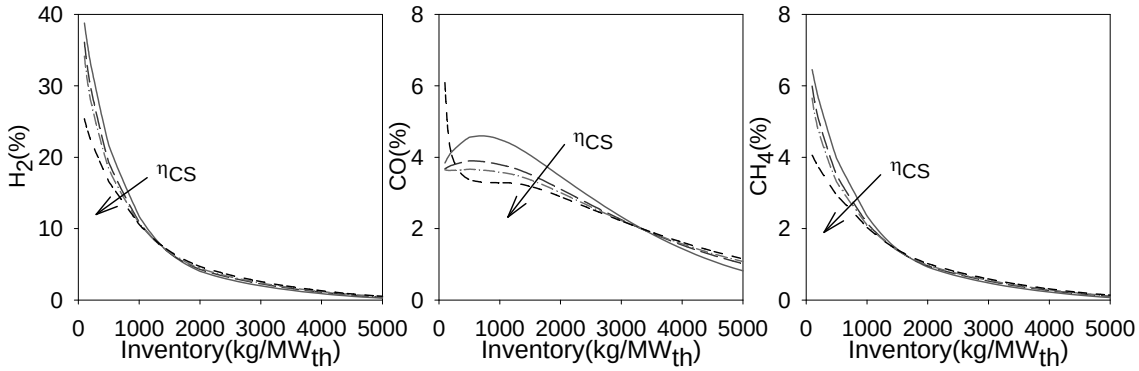

Fig. 11. Variation of H_2, CO and CH_4 concentrations at the fuel reactor outlet with increasing solids inventory for η_{CS}=0%, 80%, 90% and 100%. T_{FR}=950ºC. H_2O/C=0.7. ϕ=2. $X_{s,in}$= 0. $\chi_{OC,v}$=0.53%.

Theoretical approach on the CLC performance with solid fuels: optimizing the solids inventory

Ana Cuadrat, Alberto Abad*, Pilar Gayán, Luis F. de Diego, Francisco García-Labiano, Juan Adánez

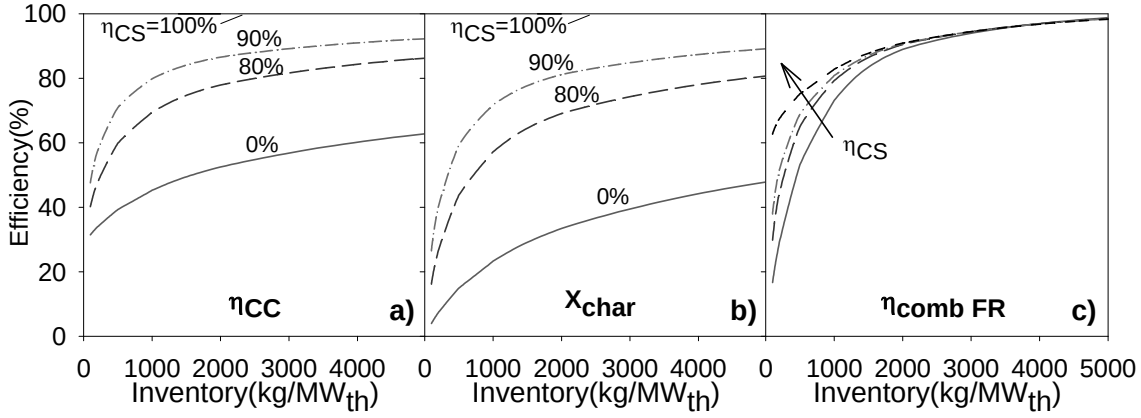

Fig. 12. Variation of a) carbon capture, b) char conversion and c) combustion efficiency with increasing solids inventory for η_{CS}=0, 80%, 90% and 100%. T_{FR}=950ºC. H_2O/C=0.7. ϕ=2. $X_{s,in}$= 0. $\chi_{OC,v}$=0.53%.

Theoretical approach on the CLC performance with solid fuels: optimizing the solids inventory

Ana Cuadrat, Alberto Abad*, Pilar Gayán, Luis F. de Diego, Francisco García-Labiano, Juan Adánez

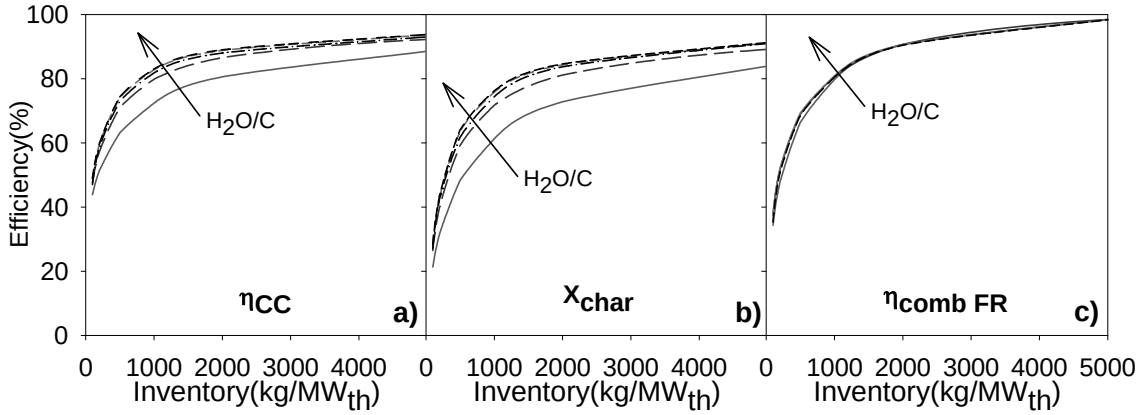

Fig. 13. Variation of a) carbon capture, b) char conversion and c) combustion efficiencies with increasing solids inventory for H_2O/C ratios of 0.4, 0.7, 2 and 4. T_{FR}=950ºC. ϕ=2. η_{CS}=90%. $X_{s,in}$= 0. $\chi_{OC,v}$=0.53%.

Theoretical approach on the CLC performance with solid fuels: optimizing the solids inventory

Ana Cuadrat, Alberto Abad*, Pilar Gayán, Luis F. de Diego, Francisco García-Labiano, Juan Adánez

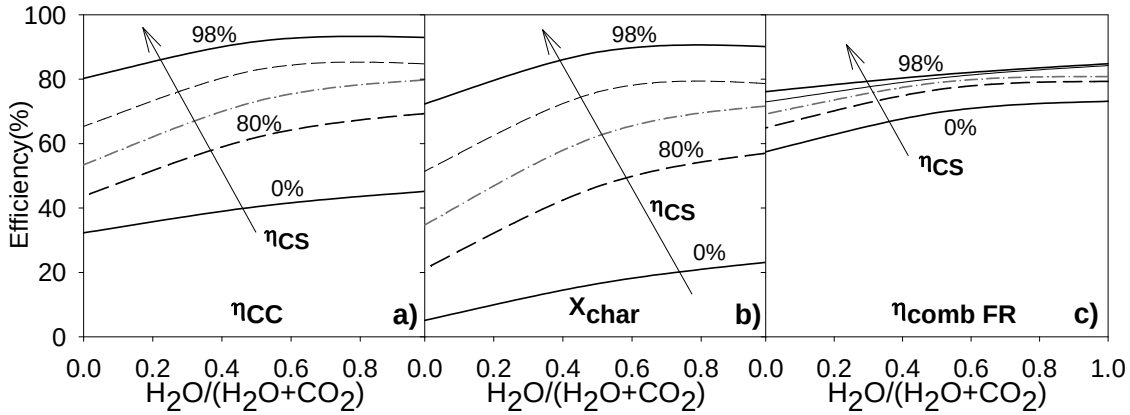

Fig. 14. Variation of a) carbon capture, b) char conversion and c) combustion efficiencies with different H_2O:CO_2 mixtures as gasification agent and for several η_{CS}: 0%, 80%, 90%, 95% and 98%. Inventory= 1000 kg/MW_{th}. T_{FR}=950ºC. (H_2O+CO_2)/C=0.7. ϕ=2. $X_{s,in}$= 0. $\chi_{OC,v}$=0.53%.

Theoretical approach on the CLC performance with solid fuels: optimizing the solids inventory

Ana Cuadrat, Alberto Abad*, Pilar Gayán, Luis F. de Diego, Francisco García-Labiano, Juan Adánez

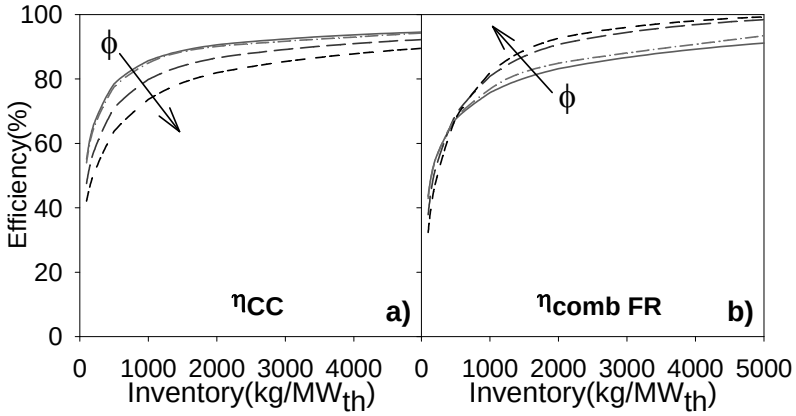

Fig. 15. Variation of a) carbon capture and b) combustion efficiencies with increasing solids inventory for oxygen carrier to fuel ratios, ϕ, of 1.1, 1.2, 1.5, 2 and 3.33. T_{FR}=950ºC. H_2O/C=0.7. η_{CS}=90%. $X_{s,in}$= 0. $\chi_{OC,v}$=0.53%.

Theoretical approach on the CLC performance with solid fuels: optimizing the solids inventory

Ana Cuadrat, Alberto Abad*, Pilar Gayán, Luis F. de Diego, Francisco García-Labiano, Juan Adánez

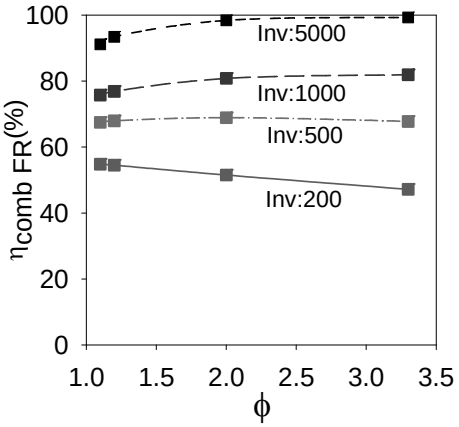

Fig. 16. Resulting combustion efficiency with increasing ϕ for inventories of 200, 500, 1000 and 5000 kg/MW_{th}. T_{FR}=950ºC. H_2O/C=0.7. η_{CS}=90%. $X_{s,in}$= 0. $\chi_{OC,v}$=0.53%.

Theoretical approach on the CLC performance with solid fuels: optimizing the solids inventory

Ana Cuadrat, Alberto Abad*, Pilar Gayán, Luis F. de Diego, Francisco García-Labiano, Juan Adánez

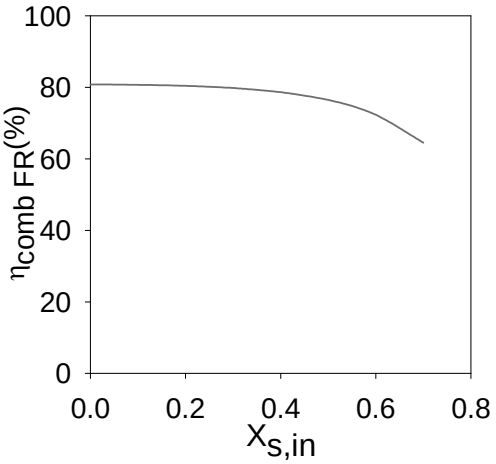

Fig. 17. Combustion efficiency variation with increasing $X_{s,in}$. Inventory = 1000 kg/MW_{th}. T_{FR}=950ºC. H_2O/C=0.7. ϕ=2. η_{CS}=90%. $\chi_{OC,v}$=0.53%.

Theoretical approach on the CLC performance with solid fuels: optimizing the solids inventory

Theoretical approach on the CLC performance with solid fuels: optimizing the solids inventory

Ana Cuadrat, Alberto Abad*, Pilar Gayán, Luis F. de Diego, Francisco García-Labiano, Juan Adánez

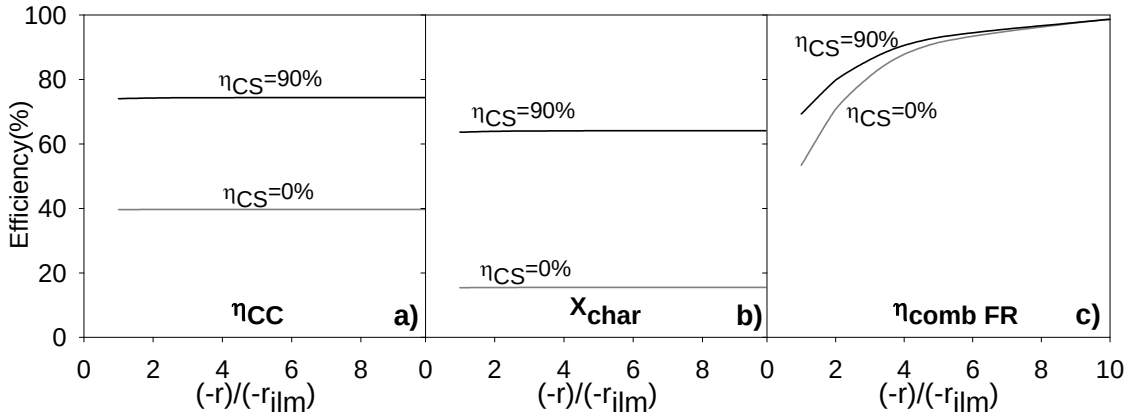

Fig. 18. Variation of a) carbon capture, b) char conversion and c) combustion efficiency with increasing oxygen carrier reaction rate, for carbon stripper efficiencies of 0% and 90%. Inventory=500 kg/MW_{th}. T_{FR}=950ºC. H_2O/C=0.7. ϕ=2. $X_{s,in}$= 0.

Theoretical approach on the CLC performance with solid fuels: optimizing the solids inventory

Ana Cuadrat, Alberto Abad*, Pilar Gayán, Luis F. de Diego, Francisco García-Labiano, Juan Adánez

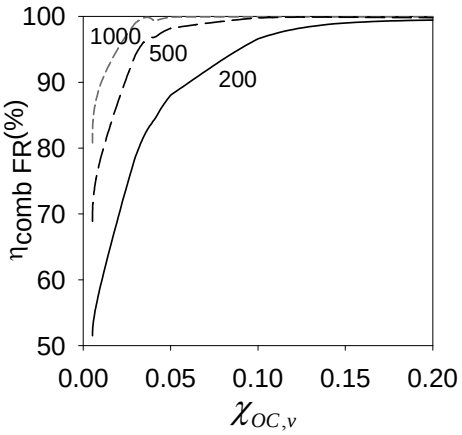

Fig. 19. Combustion efficiency variation with increasing $\chi_{OC,v}$ for several inventories: —— 200 kg/MW_{th}, ---- 500 kg/MW_{th} and ····· 1000 kg/MW_{th}. T_{FR}=950ºC. H_2O/C=0.7. ϕ=2. η_{CS}=90%. $X_{s,in}$= 0.

Theoretical approach on the CLC performance with solid fuels: optimizing the solids inventory

Ana Cuadrat, Alberto Abad*, Pilar Gayán, Luis F. de Diego, Francisco García-Labiano, Juan Adánez

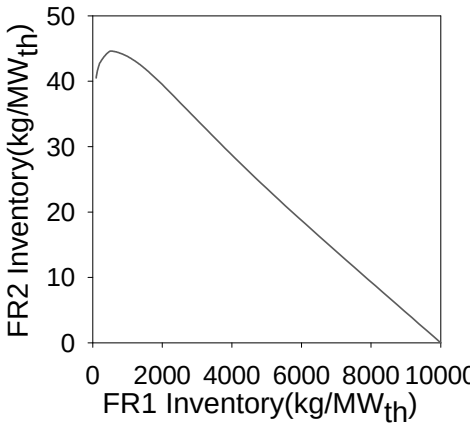

Fig. 20. Minimum ilmenite inventory in the second fuel reactor to completely oxidize the fuel for different inventories in the first fuel reactor. T_{FR}=950ºC. Conditions in the first fuel reactor: H_2O/C=0.7. ϕ=2. η_{CS}=90%. $X_{s,in}$= 0. $\chi_{OC,v}$=0.53%.